The stable carbon and hydrogen isotopic composition of microbial fatty acids traces microbial metabolism in soils and peats

Yiming Zhang [a,b,c], B. David A. Naafs [c], Xianyu Huang [a,b,*], Meiling Zhao [b,l], Linghan Zeng [b], Jerome Blewett [d,c], Richard D. Pancost [c], Shucheng Xie [a]

[a] *State Key Laboratory of Biogeology and Environmental Geology, China University of Geosciences, Wuhan 430078, China*

[b] *Laboratory of Critical Zone Evolution, School of Geography and Information Engineering, China University of Geosciences, Wuhan 430078, China*

[c] *Organic Geochemistry Unit, School of Chemistry, and School of Earth Sciences, University of Bristol, Bristol BS8 1TS, UK*

[d] *Department of Earth and Planetary Sciences, Harvard University, Cambridge, MA, USA*

[*] *Corresponding author: xyhuang@cug.edu.cn*

[l] *Present address: Key Laboratory of Wetland Ecology and Environment, Northeast Institute of Geography and Agroecology, Chinese Academy of Sciences, Changchun 130102, China*

ABSTRACT

The compound-specific stable carbon ($\delta^{13}C$) and hydrogen ($\delta^{2}H$) isotopic compositions of microbial fatty acids have been widely used to trace microbial metabolism across a range of mesophilic environments. However, few studies have combined the $\delta^{13}C$ and $\delta^{2}H$ values of microbial fatty acids. So far none have determined the $\delta^{2}H$ of microbial phospholipid fatty acids (PLFAs) in soils or peats, even though these stable isotope combinations could provide new insights into soil microbial metabolism. Here, we measured the $\delta^{13}C$ and $\delta^{2}H$ values of microbial PLFAs in top soils from peatlands, meadows, and woodlands in the Dajiuhu basin, central China. We observed a significant ($p < 0.05$) positive correlation between the $\delta^{13}C$ and $\delta^{2}H$ of microbial PLFAs across the three habitats studied here, indicating that central metabolic pathways affect both carbon and hydrogen isotopic compositions of microbial PLFAs. Moreover, our stable isotope data consistently indicate a relatively conservative metabolic state, which is dominated by expected heterotrophic metabolism. The exception to these observations is PLFAs associated with methanotrophs, as these appear to have decoupled carbon and hydrogen isotopes, providing an additional tool for tracing methanotrophic signals. Our results suggest that the carbon and hydrogen dual isotopic composition of microbial PLFAs can not only provide cross-validation for microbial metabolism in natural environments, but as a combined tool can also provide new insights into the perturbation of soil microbial community metabolism.

Keywords: $\delta^{13}C$; $\delta^{2}H$; isotopic composition; fatty acids; soil microbial metabolism

1. INTRODUCTION

Microorganisms are critical drivers of Earth's carbon, nitrogen, sulfur, and other elemental cycles. Identifying and understanding microbial metabolic activity is critical to assessing microbial function and its feedback to the environment (Bardgett et al., 2008; Jansson and Hofmockel, 2020). Microbial membrane lipids and their compound-specific isotopic compositions provide an effective tool for *in situ* identification of microbial communities and metabolic activities (Vestal and White, 1989; Boschker and Middelburg, 2002; Pancost and Sinninghe Damsté, 2003; Lengger et al., 2019; Blewett et al., 2022). The isotopic signals of microbial lipids preserved in sediments can also be used to reconstruct past biogeochemical processes (Hayes et al., 1990; Pancost et al., 2007; van Winden et al., 2012; Elvert et al., 2016; Talbot et al., 2016; Naafs et al., 2019; Blewett et al., 2022).

Among the wide range of microbial lipids, fatty acids are fundamental components of the cell membrane phospholipid bilayer. They are biosynthesized by bacteria and eukaryotes and are the biosynthetic precursors for other *n*-alkyl lipids (Ohlrogge and Browse, 1995; Schirmer et al., 2010; Sachse et al., 2012). Cell membrane phospholipid-derived fatty acids (PLFAs) are representative of the living microbial community, as phospholipids degrade rapidly (hours to days) after cell death (White et al., 1979; Kindler et al., 2009; Dippold and Kuzyakov, 2016; Zhang et al., 2019). The diversity in the structure of PLFAs is empirically linked to broad groups of soil microbiota such as Gram-negative and Gram-positive bacteria (e.g., Zelles, 1999; Hill et al., 2000; Frostegård et al., 2011). On this basis, the stable carbon and hydrogen isotopic

compositions of microbial PLFAs have been used to track substrate utilization and metabolic activities across microbial communities (e.g., Zhang et al., 2004; Evershed et al., 2007; Brady et al., 2010; Watzinger, 2015; Heinzelmann et al., 2018).

The stable carbon isotopic composition ($\delta^{13}C$) of PLFAs has been studied and applied particularly extensively. The $\delta^{13}C$ values of microbial fatty acids are predominantly controlled by the $\delta^{13}C$ of the substrate and kinetic isotope effects (KIEs) during microbial carbon assimilation and fatty acid biosynthesis (Monson and Hayes, 1982; Hayes, 1993, 2001; Pancost and Sinninghe Damsté, 2003). Laboratory incubation experiments have found that heterotrophic microbes are characterized by a smaller carbon isotopic fractionation ($\varepsilon C_{FA/substrate}$) between their fatty acids and substrate (Monson and Hayes, 1982; Blair et al., 1985; Abraham et al., 1998; Cowie et al., 2009) compared to autotrophs and methanotrophs that produce more ^{13}C-depleted lipids (Summons et al., 1994; Sakata et al., 1997; Jahnke et al., 1999, 2001; van der Meer et al., 1998, 2001; Zhang et al., 2003; Londry et al., 2004, 2008; Schouten et al., 2004). As a result, the isotopic fractionation signature of fatty acids has been investigated in many natural environments, including soils and marsh sediments (Boschker et al., 1999; Cifuentes and Salata, 2001; Burke et al., 2003; Pelz et al., 2005; Stemmer et al., 2007; Watzinger et al., 2008, 2014), hot spring (Zhang et al., 2004; Pancost et al., 2006; Naraoka et al., 2010), underground aquifers (Fang et al., 2006; Mills et al., 2010; Simkus et al., 2016), rocks (Petsch et al., 2003; Seifert et al., 2013; Ziolkowski et al., 2013; Brady et al., 2018), lake sediments (Brady et al., 2010, 2014; Chen et al., 2019),

and marine sediments (Cifuentes and Salata, 2001; Zhang et al., 2002, 2005), and they have provided a wealth of information on microbial carbon metabolism in these settings.

Compared to carbon isotopes, the hydrogen isotopic composition (δ^2H) of microbial fatty acids is relatively poorly studied. Unlike carbon, the stable hydrogen isotopic composition of microbial fatty acids is mainly controlled by the δ^2H of the source water and nicotinamide adenine dinucleotide phosphate (NADPH) metabolism rather than that of the substrate (Saito et al., 1980; Sessions et al., 1999, 2002; Valentine et al., 2004; Campbell et al., 2009; Zhang et al., 2009; Valentine, 2009; Wijker et al., 2019). For instance, fatty acids produced by heterotrophic bacteria are only modestly depleted or even enriched in ^2H relative to source water, with hydrogen isotope fractionation ($\varepsilon H_{FA/water}$) between fatty acids and source water ranging from -150 ‰ to +400 ‰ (Zhang et al., 2009; Dirghangi and Pagani, 2013; Fang et al., 2014; Heinzelmann et al., 2015a, 2015b; Wijker et al., 2019). In contrast, fatty acids produced by photo- and chemoautotrophs are more depleted in ^2H, with $\varepsilon H_{FA/water}$ ranging from -220 ‰ to -160 ‰ and -400 ‰ to -250 ‰, respectively (Sessions et al., 1999; Valentine et al., 2004; Campbell et al., 2009, 2017; Zhang et al., 2009; Heinzelmann et al., 2015a, 2015b; Leavitt et al., 2016, 2017; Osburn et al., 2016). This difference suggests that the δ^2H of microbial fatty acids could be used to trace microbial metabolic activities in natural environments, such as ocean, lake, and hot spring sediments (Sessions et al., 1999; Jones et al., 2008; Li et al., 2009; Naraoka et al., 2010; Osburn et al., 2011; Dawson et al., 2015; Heinzelmann et al., 2016, 2018; Ladd et al., 2017, 2018; Zhao et al., 2020a;

107 Chen et al., 2021). However, to our knowledge, the δ^2H of microbial PLFAs has not
108 been reported from soils and peats.

109 Even though a few studies have adopted a dual carbon and hydrogen compound-
110 specific isotope approach (Huang et al., 2005; Naraoka et al., 2010; Feakins et al., 2018;
111 He et al., 2022; McFarlin et al., 2023), paired data for $\delta^{13}C$ and δ^2H of microbial lipids
112 are very scarce. Theoretically, both the $\delta^{13}C$ and δ^2H of microbial lipids are impacted
113 by microbial metabolism, the former through the substrate and the latter through the
114 role of NADPH in lipid biosynthesis, but these are based on laboratory cultures with
115 controllable substrates that are rarely representative of the natural environment.
116 Whether δ^2H of microbial lipids can be used to track the core metabolism of microbial
117 communities in natural environments needs to be further verified (Osburn et al., 2011;
118 Dawson et al., 2015; Ladd et al., 2017; Heinzelmann et al., 2018). More importantly,
119 the relationship between microbial lipid $\delta^{13}C$ and δ^2H is unclear, especially in the
120 natural environment. Whether their combination can provide complementary or
121 contrasting metabolic information has not yet been tested, inhibiting the emergence of
122 new tools for understanding (past) key microbial metabolic processes.

123 In this study, we investigated the $\delta^{13}C$ and δ^2H values of microbial PLFAs in natural
124 soil samples, including a peatland, meadow, and woodland. These data have been
125 combined with measurements of environmental parameters such as soil total organic
126 carbon content (TOC), $\delta^{13}C$ of bulk soil organic carbon ($\delta^{13}C_{bulk}$), soil water δ^2H
127 (δ^2H_{water}), soil water content (SWC), soil pH, and nutrients. Our objectives are to
128 explore (1) the characteristics of $\delta^{13}C_{PLFA}$ and δ^2H_{PLFA} and their offsets with $\delta^{13}C_{bulk}$

($\varepsilon C_{FA/bulk}$) and δ^2H_{water} ($\varepsilon H_{FA/water}$) in natural peats and soils, (2) the relationship between $\delta^{13}C_{PLFA}$ ($\varepsilon C_{FA/bulk}$) and δ^2H_{PLFA} ($\varepsilon H_{FA/water}$) and constrain whether they reflect similar, complementary, or contrasting metabolic information, and (3) the impacts of lipid biosynthetic pathway and environmental parameters on the isotopic offset of microbial PLFAs across these contrasting environments.

2. MATERIALS AND METHODS

2.1. Study site and sampling

Samples were collected from the Dajiuhu basin (31°25′~31°32′ N, 109°58′~110°08′ E), a closed subalpine basin with an average altitude of 1730 m above sea level (Huang et al., 2018). This basin has diverse habitats, including natural peatlands, meadows, broadleaf deciduous woodlands, rivers, and (artificial) shallow lakes (Fig. 1). Due to its importance to biodiversity, this area has been a national park and was adopted into the list of Wetland of International Importance (Ramsar List) and the World Wildlife Fund Global 200.

Subtropical humid monsoon climate predominates in this region, with a mean annual rainfall of 1560 mm and a mean annual temperature of 7.2 ℃ (Huang and Meyers, 2019). The dominant vegetation in the peatlands includes *Sphagnum palustre*, *Carex argyi*, *Sanguisorba officinalis*, and *Euphorbia esula* (Luo et al., 2015). In meadows, *Carex argyi* and *Juncus effusus* are the dominant species under wetter conditions, while *Anaphalis sinica*, *Fragaria orientalis,* and *Scirpus karuizawensis* become abundant under drier conditions (Luo et al., 2015). In woodlands, *Quercus aliena* var.

acuteserrata and *Malus hupehensi* become important (Li et al., 2007; Yan et al., 2020).

During a field campaign in June 2018, two transects across different habitats were set following a previous investigation into the vegetation (Luo et al., 2015). A total of 22 topsoil samples (0-5 cm) were collected across these transects, including samples from peatland, meadow, and deciduous woodland habitats (Fig. 1). The samples were quickly transported to the laboratory and preserved in a freezer before further treatment.

2.2. Soil environmental and bulk geochemical analysis

Soil temperature was measured during the field campaign with a HQ40d portable meter (Hach, U.S.A.). Soil water content (SWC) was calculated by comparing the weight of fresh samples versus that after freeze-drying. Soil pH was measured on a mixture of soil and water (1:5, v:v). The freeze-dried and ground soil sample was immersed in deionized water for 30 min. The solution was centrifuged (4000 rpm/min) for 3 min. The supernatant was collected to measure the pH value using a HQ40d portable meter (Hach, U.S.A.).

The concentration of NH_4^+-N and NO_3^--N was analyzed using a San++ continuous flow analyzer (Sakalar Analytical B.V.). A fresh soil sample of ca. 3 g was added to a centrifuge tube, then 30 mL KCl (1 mol/L) was added. The solution was mixed using a shaker for 1 h, and then centrifuged (2500 rpm/min) for 10 min. Then 2 mL supernatant was mixed with 8 mL KCl (1 mol/L) and run on the continuous flow analyzer.

Soil TOC, C/N, and $\delta^{13}C_{bulk}$ were analyzed using a Flash EA2000 elemental analyzer coupled to a Finnigan MAT253 isotope ratio mass spectrometer. Freeze-dried samples

were ground and sieved through a 200-mesh sieve, then HCl was added to remove carbonate. The sample was freeze-dried again, then ca. 40-60 mg dried sample was packed into tin cups and analyzed. A replicate sample was measured for every six samples to monitor combustion efficiency. Reproducibility was better than 0.2 ‰. Two standards of GBW04407 ($\delta^{13}C$ = -22.4 ‰) and GBW04408 ($\delta^{13}C$ = -36.9 ‰) were used to calibrate the $\delta^{13}C$ data (more details about the two standards can be found here https://www.ncrm.org.cn/English/CRM/pdf/GBW04407_20160301_09391399_873003.pdf). Blank correction is performed by burning tin cups without samples. We controlled the injection volume to ensure that the peak amplitude (range 1-6 V) of the sample was similar to that of the standards. $\delta^{13}C$ results are reported in the δ notation (‰) relative to the Vienna Peedee Belemnite (VPDB) standard.

Soil water was extracted using a LI-2100 cryogenic vacuum extraction system (LICA United Technology Limited, China). The $\delta^{2}H$ of soil water was analyzed using an IWA-35-EP liquid water isotope analyzer (Los Gatos Research, U.S.A.). Reproducibility was better than 1 ‰. $\delta^{2}H$ results are reported in the δ notation (‰) relative to the Vienna Standard Mean Ocean Water (VSMOW) standard.

2.3. Lipid extraction

Freeze-dried soil samples were ground and sieved through a 60-mesh sieve. Fresh plant material was removed to minimize the influence of plant-derived PLFAs. A modified Bligh and Dyer method was applied to extract phospholipids (Bligh and Dyer, 1959; White et al., 1979). Briefly, 5 g of ground soil was immersed in a mixture of

195 dichloromethane (DCM), methanol, and phosphate buffer (1:2:0.8, v:v) and
196 ultrasonically extracted for 15 min. The solution was then centrifuged (4000 rpm/min)
197 for 4 min, and the supernatant was transferred into a separatory funnel. Additional DCM
198 and ultrapure water were added into the separatory funnel to modify the solvent ratio to
199 1:1:0.9 (DCM: methanol: phosphate buffer). The mixture was shaken vigorously and
200 left overnight, and the prior homogenous mixture gradually changed to a lower organic
201 phase and an upper aqueous phase. The organic phase was collected and concentrated
202 to obtain the total lipid extract (TLE). The TLE was then separated into neutral lipid,
203 glycolipid, and phospholipid fractions using silica gel column chromatography with
204 eluents of DCM+2% acetic acid (Dickson et al., 2009), acetone, and methanol,
205 respectively.

206 The phospholipid fraction was derivatized to yield phospholipid fatty acid methyl
207 esters (FAMEs) using mild alkaline methanolysis (Dowling et al., 1986). An internal
208 standard (*n*-C_{19} fatty acid) was added for quantification before the transesterification,
209 for which methanolic potassium hydroxide solution (0.2 mol/L) was added to the
210 phospholipid fraction. The mixture was capped and heated at 37 °C for 15 min. After
211 cooling to room temperature, acetic acid was added to neutralize the solution. Then *n*-
212 hexane and double distilled water were added and mixed vigorously to allow separation.
213 The upper phase (hexane) containing the FAMEs was transferred by pipette. *n*-Hexane
214 was added three times, and the upper phases were combined and dried under a gentle
215 nitrogen stream.
216

2.4. GC-MS analysis

FAMEs were analyzed using a HP 6890 gas chromatograph equipped with a HP 5973 mass selective detector (GC-MS) and a DB-5 MS capillary column (30 m × 0.25 mm internal diameter, 0.25 μm film thickness). The GC oven temperature was programmed as follows: the initial temperature was set at 50 °C (1 min hold), increased to 210 °C at 2 °C/min, and then increased to 310 °C at 4 °C/min (15 min hold). Compounds were identified by comparison with published mass spectra (Jensen and Gross, 1987), retention times of a FAMEs standard mixture (Supelco, 47885-U and 47080-U), and MIDI identification software (MIDI Inc., Newark, Delaware, U.S.A.). The position of double bonds of monounsaturated fatty acids was determined by dimethyl disulfide derivatization following the method from Nichols et al. (1986).

2.5. GC-C-IRMS analysis

Compound-specific $\delta^{13}C$ analysis of the FAMEs was conducted using a Finnigan Trace GC coupled with a Finnigan Delta XP isotope ratio mass spectrometer equipped with a DB-5MS column (60 × 0.25 mm internal diameter, film thickness 0.25 μm). The GC oven temperature was programmed from 50 °C (1 min hold) to 210 °C (2 min hold) at 10 °C/min, then increased to 300 °C (2 min hold) at 4 °C/min, and finally increased to 310 °C (25.5 min hold) at 10 °C/min. The temperature of the oxidation oven was set at 950 °C. Squalane ($\delta^{13}C$ = -19.8 ‰) was used as an internal standard. Instrument reliability and stability were evaluated for every two samples (four analyses) using a mixture of FAMEs (*n*-C_{14}, *n*-C_{16}, *n*-C_{18}, and *n*-C_{20}) with known $\delta^{13}C$ values (from

239 Indiana University). Results are reported in the δ notation (‰) relative to the VPDB
240 standard. Reproducibility of the $\delta^{13}C$ values was better than 0.5 ‰, based on duplicate
241 analyses. We controlled the injection volume by the dilution of samples to ensure that
242 the peak amplitude (0.5 ~ 4 V) of the FAME analytes was similar to that of the standards.
243 We also discarded isotope data for any compounds with peak amplitude below 0.5 V.
244 To correct for the addition of a methyl carbon during transesterification, we used the
245 following mass balance equation:

246 $$\delta^{13}C_{PLFA} = [(n+1) \times \delta^{13}C_{FAME} - \delta^{13}C_{methanol}]/n$$

247 where *n* is the carbon number of fatty acids, $\delta^{13}C_{FAME}$ is the measured $\delta^{13}C$ value of
248 fatty acid methyl esters, and $\delta^{13}C_{methanol}$ is the $\delta^{13}C$ value of the methanol used for the
249 transesterification, which is calculated by derivatizing phthalic acid with known $\delta^{13}C$
250 (provided by Dr Arndt Schimmelmann, Indiana University).

251

252 2.6. GC-TC-IRMS analysis

253 Compound-specific $\delta^{2}H$ analysis of FAMEs was conducted using a Finnigan Trace
254 GC coupled with a Delta V Advantage isotope ratio mass spectrometer equipped with
255 a DB-5MS column (60 × 0.25 mm internal diameter, film thickness 1.0 μm). The GC
256 oven program was identical to that of the carbon isotopic analysis. The high-
257 temperature conversion oven had a temperature of 1400 °C. Squalane ($\delta^{2}H$ = -167 ‰)
258 was used as an internal standard. Instrument reliability and stability were checked using
259 a mixture of FAMEs (*n*-C_{14}, *n*-C_{16}, *n*-C_{18}, and *n*-C_{20}) with known $\delta^{2}H$ values (from
260 Indiana University). Results are reported in the δ notation (‰) relative to the VSMOW

standard. Reproducibility of the δ^2H values was better than 5 ‰ based on duplicate analyses. The H_3^+ factor was measured daily with peak heights varying from 1 to 7 V, which had an average of 3.54 ppm/mV (range from 3.46 to 3.68) during the measurement period. We controlled the injection volume by the dilution of samples to ensure that the peak amplitude (1 ~ 4 V) of the FAME analytes was similar to that of the standards. We also discarded isotope data for any compounds with peak amplitude below 1V. To correct for the addition of hydrogen during the transesterification, the following mass balance equation was used:

$$\delta^2H_{PLFA} = [(2n+2) \times \delta^2H_{FAME} - 3\times\delta^2H_{methanol}]/(2n-1)$$

Where *n* is the carbon number of fatty acids, δ^2H_{FAME} is the measured δ^2H value of fatty acid methyl esters, and $\delta^2H_{methanol}$ is the δ^2H value of the methanol used for the transesterification, which is calculated by derivatizing phthalic acid with known δ^2H as described by Session (2006).

2.7. Isotopic offset calculation and statistical analyses

The carbon and hydrogen isotopic offset of PLFAs relative to bulk organic carbon and source water were calculated as follows:

$$\varepsilon C_{FA/bulk} = \frac{\delta^{13}C_{PLFA} + 1}{\delta^{13}C_{bulk} + 1} - 1$$

$$\varepsilon H_{FA/water} = \frac{\delta^{2}H_{PLFA} + 1}{\delta^{2}H_{water} + 1} - 1$$

280 The results were multiplied by the factor of 1,000 and reported as per mil (‰) (Coplen
281 et al., 2011; Sachse et al., 2012). Another commonly used term, the fractionation factor
282 α, can be related to the ε by:

283 $$\varepsilon = \alpha - 1$$

284 The factor lambda (Λ) is defined by the slope of the linear regression for carbon and
285 hydrogen dual isotope discrimination (Elsner et al., 2007; Feisthauer et al., 2011):

286 $$\Lambda = \frac{\alpha_H^{-1} - 1}{\alpha_C^{-1} - 1}$$

287 The Λ term was originally defined as a specific reaction in which the isotopic effects of
288 carbon and hydrogen are both due to the same enzymatic process. In our samples, the
289 fractionation values represent the average of different microorganisms and different
290 enzymatic reaction processes in the natural environments. Therefore, we refer to the
291 mathematically identical 'correlation slope' instead of Λ in the following text.

292 To test whether there are significant differences in environmental parameters and
293 microbial composition in the three habitats, variance analysis (ANOVA) and cluster
294 analysis were performed using the IBM SPSS Statistics 25.0 software. Correlation
295 analysis was performed using the R 4.1.2 software with the "corrplot" package (Wei
296 and Simko, 2021). The results were expressed using Pearson correlation coefficients (r)
297 and significance p values.

298

299 **3. RESULTS**

300 3.1. Soil environmental parameters and bulk geochemistry

The soil environmental and bulk geochemical parameters differ across the three habitats. The soil water content of the peatland was avg. 86 %, significantly higher than that of meadow and woodland (avg. 42 % and 48 %) (one-way ANOVA, $p < 0.001$) (Table 1). The pH from all habitats was acidic, with peatlands having a lower pH (avg. 4.0) compared to meadows and woodlands (one-way ANOVA, $p < 0.05$) (Table 1). The nitrate content (NO_3^--N) of the meadow (avg. 0.65) was significantly higher than that of the peatland and woodland (avg. 0.11 and 0.08, respectively) (one-way ANOVA, $p = 0.01$), whereas the ammonium content (NH_4^+-N) was similar among the three habitats (one-way ANOVA, $p = 0.68$) (Table 1). The soil temperature was similar across the three habitats (one-way ANOVA, $p = 0.2$) (Table 1).

The peatland samples had significantly higher TOC contents (avg. 19.5 %) than the meadow and woodland samples (one-way ANOVA, $p < 0.001$) (Table 1), which were not statistically different (avg. 6.1 and 9.1 %, respectively). The soil C/N ratio in the woodland (avg. 25.2) was higher than that in the peatland and meadow (avg. 17.2 and 17.2, respectively) (one-way ANOVA, $p < 0.05$) (Table 1). The δ^2H_{water} values were significantly (one-way ANOVA, $p < 0.01$) different among the three habitats, with the meadow (avg. -49.2 ‰) and woodland (avg. -52.9 ‰) having lower values compared to the peatland (avg. -39.9 ‰) (Table 1). The $\delta^{13}C_{bulk}$ values were similar across the three habitats, with an average value of ca. -28 ‰ ($1\sigma = 0.7$) (Table 1).

3.2. Abundance and composition of PLFAs

322 Our previous work has reported the molecular distribution of PLFAs in these soil
323 samples (Zhao et al., 2020b). Briefly, 22 types of PLFAs with carbon numbers from C_{14}
324 to C_{19} were identified. The average total PLFA concentration of surface peat (avg. 270
325 μg/g) was an order of magnitude higher than that of the meadow and woodland samples
326 (avg. 26 μg/g and 33 μg/g, respectively). Overall, 16:0 is dominant (avg. 17.6 %),
327 followed by 18:1ω7c (avg. 12.7 %), i15:0 16:1ω7c, 10Me16:0, 18:1ω9c, and cy19:0
328 occupying more than 5 %. When grouped according to molecular structure,
329 monounsaturated PLFAs are dominant (33.8 %), followed by straight-chain saturated
330 PLFAs (26.1 %), terminally branched PLFAs (20.7 %), cyclopropyl PLFAs (10.4 %),
331 and 10-methyl branched PLFAs (9 %). Polyunsaturated PLFAs account for only a small
332 percentage (1.3 %) of the total PLFAs.
333 PLFA classification is based on previous studies on the composition and changes of
334 soil microbial communities (e.g., Frostegård and Bååth, 1996; Bossio and Scow, 1998;
335 Hill et al., 2000; Zelles, 1999; Jaatinen et al., 2007); however, caution is needed as some
336 PLFAs have multiple microbial origins (Frostegård et al., 2011). For example, 18:1ω9c
337 is considered to be a fungal marker when its abundance has a significant positive
338 correlation with 18:2ω6,9c; otherwise, it is assigned as a bacterial marker (Frostegård
339 et al., 2011). In our samples, the abundance of 18:2ω6,9c is low, accounting for only
340 1.3 % of the total PLFAs, and no significant correlation was found between the
341 fractional abundance of 18:1ω9c and 18:2ω6,9c ($r^2 = 0.03$, $p = 0.48$), suggesting a major
342 bacterial origin of 18:1ω9c. Moreover, although we removed fresh plant material to
343 minimize the influence of plant-derived PLFAs, the input of plant material cannot be

completely removed from soil samples, for example as fine roots. Nonetheless, plants have a large amount of polyunsaturated PLFAs, such as 18:2ω6,9c and 18:3ω3,6,9c (Zelles, 1997), and these are rare in our samples, e.g., 18:3ω3,6,9 was not detected. This suggests that input from plant-derived PLFAs is negligible. Kaiser et al. (2010) also showed that the contribution of roots to soil PLFAs can be negligible.

Assuming specific PLFAs can be assigned to certain bacterial or fungal groups, the microbial community structure of surface peat was different from that of the meadow and woodland (Fig. 2). Compared with the meadow and woodland, there were more G– and fewer G+ bacteria in the peatland. However, the variability between different samples within the peatland was significant (Fig. 2), and cluster analysis is not entirely diagnostic, which groups some of the peatland PLFA-producing microbial communities with those found in the meadow and woodland samples (Fig. 2).

3.3. Carbon isotopic composition of PLFAs

The $\delta^{13}C$ values of 15 different types of PLFAs were determined (Fig. 3a). The concentrations of the other PLFAs were insufficient to obtain reliable isotopic measurements. Across all samples, the individual $\delta^{13}C$ values ranged from -20.6 to -40.4 ‰, with average values for each fatty acid between -24 and -34 ‰ (Fig. 3a). The meadow and woodland sites shared similar $\delta^{13}C$ values (-20 ‰ ~ -31 ‰), most of which were higher than $\delta^{13}C_{bulk}$ (Fig. 3a). In contrast, PLFAs from peatlands were significantly more depleted (-26 ‰ ~ -40 ‰) (one-way ANOVA, $p < 0.001$), especially those PLFAs

365 derived from G– bacteria (Fig. 3a). For example, the average $\delta^{13}C$ value of the 16:1ω7c,
366 18:1ω7c, and cy19:0 fatty acids was below -32 ‰, with minima that reached -40 ‰.
367 The offset between the $\delta^{13}C$ of PLFAs and bulk organic carbon ($\varepsilon C_{FA/bulk}$) ranged
368 from +8.8 to -12.3 ‰. In the meadow and woodland samples, average $\varepsilon C_{FA/bulk}$ values
369 were all > 0 ‰ except for cy19:0 (Fig. 3b). For peatlands, the average $\varepsilon C_{FA/bulk}$ values
370 were significantly lower (one-way ANOVA, $p < 0.001$), being close to 0 ‰ for most
371 PLFAs (Fig. 3b), less than -3 ‰ on average for the 16:1ω7c, 18:1ω7c, and cy19:0 (Fig.
372 3b), and reaching -12 ‰ for some individual PLFAs.
373
374 3.4. Hydrogen isotopic composition and offset of PLFAs
375 The $\delta^{2}H$ values of the individual PLFAs ranged from -87 to -234 ‰ across all
376 samples. The average $\delta^{2}H$ values were similar across the three habitats (Fig. 4a), except
377 for i17:0, a17:0, and 10Me18:0. Most $\delta^{2}H$ values varied between -140 and -200 ‰ (Fig.
378 4a); however, the average $\delta^{2}H$ values of a15:0, 18:1ω7c, cy19:0, and 10Me18:0 were
379 more depleted, with minima as low as -230 ‰ (Fig. 4a).
380 The offset between $\delta^{2}H$ of PLFAs and water ($\varepsilon H_{FA/water}$) in all samples ranged from -
381 52 to -206 ‰, with average values for each lipid ranging between -90 and -180 ‰ (Fig.
382 4b). The $\varepsilon H_{FA/water}$ values of most PLFAs were similar across all habitats (Fig. 4b), and
383 most $\varepsilon H_{FA/water}$ values were > -160‰ (Fig. 4b), except for a15:0, a17:0, 18:1ω7c, cy19:0,
384 and 10Me18:0. The $\varepsilon H_{FA/water}$ values of these fatty acids were as low as -200 ‰ (Fig.
385 4b).
386

3.5. Relationship between carbon and hydrogen isotopes of PLFAs

Statistical analysis of all samples shows that there is a significant correlation between $\delta^{13}C$ ($\varepsilon C_{FA/bulk}$) and $\delta^{2}H$ ($\varepsilon H_{FA/water}$) of individual PLFA (Fig. 5). For example, the $\delta^{13}C$ ($\varepsilon C_{FA/bulk}$) values of straight-chain saturated PLFAs (16:0 and 18:0), terminal branched PLFAs (i15:0, a15:0, i16:0, i17:0, a17:0), and monounsaturated 16:1ω7c, are significantly ($p < 0.05$) positively correlated with their $\delta^{2}H$ ($\varepsilon H_{FA/water}$) values (Fig. 5 and Figs. 6a, 6b, 6c). There is no significant (one-way ANOVA, $p > 0.05$) difference in the slope of linear regression between these PLFAs. However, for other PLFAs, such as 18:1ω7c and 18:1ω9c, their $\delta^{13}C$ ($\varepsilon C_{FA/bulk}$) is not correlated with $\delta^{2}H$ ($\varepsilon H_{FA/water}$) (Fig. 5 and Fig. 6c).

Dividing all samples by habitat, there is a relatively weak but significant ($p < 0.05$) positive correlation between $\delta^{13}C_{PLFA}$ and $\delta^{2}H_{PLFA}$ values in all three habitats (Fig. 6d). The $\varepsilon C_{FA/bulk}$ and $\varepsilon H_{FA/water}$ also have significant ($p < 0.01$) positive correlations in peatland and meadow samples (Fig. 6e). There is no significant correlation ($p > 0.05$) between $\varepsilon C_{FA/bulk}$ and $\varepsilon H_{FA/water}$ in woodland.

Based on parallel data of $\varepsilon C_{FA/bulk}$ and $\varepsilon H_{FA/water}$, we further calculated the correlation slope of the linear regression for carbon and hydrogen dual isotope discrimination across our three habitats. The correlation slopes in peatland, meadow, and woodland are 5.9 ($\pm$ 1.3), 6.4 (±2.2), and 6.2 (±3.2), respectively (Fig. 6f), not statistically different (one-way ANOVA, $p > 0.05$).

3.6. Correlation between PLFAs isotope and environmental parameters

409 The $\delta^{13}C_{PLFA}$ and $\varepsilon C_{FA/bulk}$ values have significant ($p < 0.05$) negative correlations
410 with soil water content and TOC (Fig. 5). There is weak but significant ($p < 0.05$)
411 positive correlations between soil pH, NO_3^--N, NH_4^+-N and $\delta^{13}C_{PLFA}$ ($\varepsilon C_{FA/bulk}$) of
412 several PLFAs (Fig. 5). No correlation is found between $\delta^{13}C_{PLFA}$ ($\varepsilon C_{FA/bulk}$) values and
413 C/N ratios (Fig. 5). Soil temperature is correlated to $\varepsilon C_{FA/bulk}$ values of two PLFAs
414 (10Me18:0 and cy17:0) (Fig. 5).

415 However, only a few PLFAs have δ^2H ($\varepsilon H_{FA/water}$) values that significantly correlate
416 with environmental parameters. For example, soil water content and TOC are positively
417 correlated with δ^2H ($\varepsilon H_{FA/water}$) values of iso- and anteiso-PLFAs, and negatively
418 correlated with δ^2H ($\varepsilon H_{FA/water}$) values of 10Me18:0 (Fig. 5).

419

420 **4. DISCUSSION**

421 4.1. Hydrogen isotope composition of soil water

422 Our δ^2H_{water} values represent a single measurement of soil water during the field
423 campaign in mid to late June 2018 (Table 1). While sampling, there was neither extreme
424 rainfall nor drying in the Dajiuhu basin (Supplementary Material Fig. S1). The average
425 daily precipitation during the sampling week was 3.6 mm/day, slightly lower than the
426 daily precipitation (4.3 mm/day) calculated from the mean annual precipitation of the
427 Dajiuhu basin (1560 mm). However, the δ^2H of soil water can vary seasonally, and it is
428 necessary to evaluate whether our δ^2H_{water} can represent the δ^2H of source water used
429 for soil microbial growth and PLFA biosynthesis. Recently, stable hydrogen isotope
430 probing of microbial PLFAs revealed slow microbial growth rates in soil, with

generation times varying from 4 to 402 days at the compound-specific level (Caro et al., 2023). Therefore, soil microbes may integrate the δ^2H_{water} signal across the whole growth season, and the long-term average δ^2H_{water} in the growing season is likely more representative of the δ^2H of source water used in microbial lipid biosynthesis.

To assess the long-term average of δ^2H_{water} in the growing season (April to October) in the Dajiuhu basin, we compared our previous monitoring data and conducted simulations based on the soil evaporation model and meteoric water δ^2H values (Fig. 7). Our three-year monitoring from 2015 to 2017 (Huang et al., 2018; Zhao et al., 2018; Huang and Meyers, 2019) showed that the average δ^2H_{water} value of the topmost 0-10 cm during the growing season in the Dajiuhu peatland was -45.8 ‰ (1σ = 12 ‰), slightly lower than the average δ^2H_{water} value we measured in June 2018 (-44.7 ‰, 1σ = 8.4 ‰) (Fig. 7a and 7b).

However, this three-year monitoring only represents the average δ^2H_{water} value during the growing season in peatlands without meadows/woodlands. Therefore, we further simulated the δ^2H_{water} during the growing season in the whole Dajiuhu basin based on the δ^2H of precipitation and soil evaporation model (Smith and Freeman, 2006) as follows:

$$\delta^2H_{ESP} = \delta^2H_{precip} + \frac{(1-h)\times(\varepsilon^* + 12.5)}{h + [(1-h)\times(P/E)]}$$

where δ^2H_{ESP} is the hydrogen isotope composition of the evaporated soil-water pool; h is the relative humidity (82.3%, Zhang et al., 2022a); P is the flux of water via precipitation (1241.9 mm, Zhang et al., 2020); E is the evaporation flux (419.3 mm, Pan et al., 2013); ε* is the equilibrium enrichment factor between liquid and vapor,

which can be calculated from α* and its equation with temperature (Horita and Wesolowski, 1994). Temperature data were obtained from our previous monitoring during the growing season in the Dajiuhu basin (13.4 °C, Zhang et al., 2020). δ^2H_{precip} is the hydrogen isotope compositions of precipitation (Fig. 7d), which was obtained from the measured values from April to October at Wuhan and Chongqing stations in the Global Network of Isotopes in Precipitation (GNIP) (IAEA/WMO, 2023), as well as calculated monthly values using the Online Isotopes in Precipitation Calculator (OIPC) (Bowen et al., 2005; Bowen, 2023) by inputting coordinates and elevation of the Dajiuhu basin.

Then, the δ^2H of bulk soil water was calculated by mixing the evaporated soil-water pool (δ^2H_{ESP}) with precipitation as follows:

$$\delta^2H_{soil\ water} = f_e \times \delta^2H_{ESP} + (1 - f_e) \times \delta^2H_{precip}$$

where f_e is the proportion of the bulk soil water that comes from the evaporated soil-water pool, which is set at 34 % according to the ratio of evaporation and precipitation fluxes.

The simulation results show that the average δ^2H value of bulk soil water in the Dajiuhu basin during the growing season is -45.6 ‰, ~ 1 ‰ lower than the average δ^2H_{water} value we used (Fig. 7a and 7c), albeit with a larger standard deviation (1σ = 23.7 ‰) (Fig. 7c). With such a broad range, it is plausible that some of the variations in the δ^2H values of microbial fatty acids are caused by seasonal and yearly fluctuations in the δ^2H of precipitation/soil water, particularly for microorganisms that grow quickly in the soil. Peat water is more ^2H-enriched compared to meadow/woodland (Table 1),

475 which could be due to the higher rate of evaporation in peatlands. Nonetheless, there is
476 no significant difference in the measured and simulated δ^2H values of soil water (one-
477 way ANOVA, $p = 0.94$) (Fig. 7a, 7b, and 7c). Moreover, we recalculated the $\varepsilon H_{FA/water}$
478 using the simulated long-term average δ^2H_{water} value (Supplementary Material Fig. S2).
479 The recalculated results are not significantly (one-way ANOVA, $p = 0.72$) different
480 from the $\varepsilon H_{FA/water}$ calculated using the measured δ^2H_{water} in this study (Fig. 4b). These
481 results suggest that the soil water collected in this study is not significantly ^2H-depleted
482 nor enriched relative to the long-term average during the growing season.
483
484 4.2. Relationship between carbon and hydrogen isotopes of PLFAs and its implications
485 There are significant ($p < 0.05$) positive correlations between PLFA carbon and
486 hydrogen isotope (Fig. 5 and Fig. 6). Although the correlation is not strong when all
487 PLFAs are plotted together ($r^2 < 0.35$; Fig. 6d and 6e), the correlation between $\delta^{13}C$
488 ($\varepsilon C_{FA/bulk}$) and δ^2H ($\varepsilon H_{FA/water}$) can be higher for individual PLFA (Fig. 5; e.g., a15:0, r^2
489 = 0.5), and there is no significant (one-way ANOVA, $p > 0.05$) difference in the linear
490 regression slope between different PLFAs (Fig. 6a and 6b), which is striking given the
491 diversity of organisms producing these compounds. A recent study conducted by Allan
492 et al. (2023) found a positive correlation between carbon and hydrogen isotopes of
493 microalgae-derived 16:0 fatty acid in marine surface, with the regression slope similar
494 to the 16:0 PLFA in our peat and soil samples (Fig. 6g and 6h). Further research is
495 necessary to determine whether this correlation is widely present in natural habitats.
496 Nonetheless, this correlation and similar regression slope suggest some common

497 controls over the stable carbon and hydrogen isotopic composition of microbial fatty
498 acids, likely metabolism (e.g., Wijker et al., 2019). Although both $\varepsilon C_{FA/bulk}$ and $\varepsilon H_{FA/water}$
499 are associated with microbial metabolic pathways, $\varepsilon H_{FA/water}$ could be affected by
500 different factors compared to $\varepsilon C_{FA/bulk}$. For example, microbial growth rate, NADPH
501 metabolic flux, and cellular residence time of NADPH are strong controls on $\varepsilon H_{FA/water}$,
502 but these need not also impact $\varepsilon C_{FA/bulk}$, causing $\varepsilon H_{FA/water}$ to be more variable (with
503 $\varepsilon H_{FA/water}$ values in cultures that can range from -400 to +400 ‰. e.g., Valentine et al.,
504 2004; Campbell et al., 2009; Zhang et al., 2009; Heinzelmann et al., 2015a, 2015b;
505 Osburn et al., 2016; Leavitt et al., 2017; Wijker et al., 2019). However, our results
506 suggest that $\varepsilon H_{FA/water}$ is still significantly correlated with $\varepsilon C_{FA/bulk}$ in natural peats and
507 soils, further supporting the dominant impact the central metabolic pathways have on
508 both the stable carbon and hydrogen isotopic fractionation of microbial fatty acids.

509 More specifically, there may be two root reasons for the correlation between the
510 carbon and hydrogen isotopes of microbial PLFAs that we report. Firstly, it could reflect
511 the fact that both systems reflect a balance between heterotrophy and autotrophy.
512 Heterotroph PLFAs are enriched in ^{2}H relative to those from autotrophs due to the larger
513 $\varepsilon_{lipid/water}$ fractionation of the latter (e.g., Zhang et al., 2009; Campbell et al., 2017).
514 Coincidentally, heterotroph PLFAs can be enriched in ^{13}C relative to autotroph PLFAs,
515 if the latter organisms are consuming ^{13}C-depleted respired soil carbon with an
516 associated fractionation (e.g., Billings and Ziegler, 2008). Because the isotope signal of
517 fatty acids in natural environments is a mixture of various metabolisms, the correlation
518 between carbon and hydrogen in fatty acids is not strong ($r^2 \leq 0.5$; Fig. 6). Secondly,

519 this covariation could be related to the metabolic flux. Instead of the mixing of a largely
520 heterotrophic bacterial population with a small but significant autotrophic one, the
521 relationship could reflect the coupling of carbon and hydrogen isotope metabolism. For
522 example, when metabolically related acetyl-CoA and NADPH have high production
523 and metabolic fluxes, both carbon and hydrogen isotope fractionation may remain small
524 (Monson and Hayes, 1982; Wijker et al., 2019) (Supplementary Material Text S1). Thus,
525 changes in metabolic fluxes could affect carbon and hydrogen isotope fractionation
526 consistently across diverse bacterial groups.

527 The correlation between the carbon and hydrogen isotope of PLFAs is not strong (r^2
528 ≤ 0.5) (Figs. 6), but this is also due to the small range of these values. Most of the data
529 is concentrated within a narrow range. For example, the $\varepsilon C_{FA/bulk}$ values are mostly
530 clustered between -5 and +5 ‰ (Figs. 3b and 6e). The $\varepsilon H_{FA/water}$ has a range of ca. 150 ‰
531 (Figs. 4b and 6e). For individual PLFAs, the $\varepsilon H_{FA/water}$ variation is generally less than
532 100 ‰ (Fig. 4b), in contrast to the wide range of culture experiments and field results
533 from lacustrine, marine, and hot spring environments (e.g., Li et al., 2009; Naraoka et
534 al., 2010; Osburn et al., 2011; Wijker et al., 2019; Chen et al., 2021). Compared to
535 lacustrine and marine sediments and particulate organic matter (avg. -170 ‰ and 180 ‰,
536 respectively), peats and soils have significantly (one-way ANOVA, $p < 0.01$) higher
537 $\varepsilon H_{FA/water}$ values (avg. -132 ‰) (Fig. 6i), indicating greater heterotroph activities. The
538 narrow range we observe indicates that soil metabolic processes are relatively constant
539 in natural systems. It also indicates the conservatism of soil microbial metabolism,
540 which is dominated by heterotrophs as expected. Thus, the perturbation of these $\delta^{13}C$

($\varepsilon C_{FA/bulk}$) and δ^2H ($\varepsilon H_{FA/water}$) values may indicate disruption of the soil microbial community. For example, a change in $\varepsilon C_{FA/bulk}$ and $\varepsilon H_{FA/water}$ values from a relatively narrow range to more variability (i.e., much higher/lower $\varepsilon C_{FA/bulk}$ and $\varepsilon H_{FA/water}$ values) may indicate a breakdown in the conservative metabolic state of soil microbes caused by disturbances such as drainage and subsequent soil degradation (e.g., Fenner et al., 2005; Jaatinen et al., 2007; Andersen et al., 2013). If so, a dual isotopic approach could be used to reflect soil health and degradation. Moreover, when using the dual isotopic signal of sedimentary microbial lipids to reflect the ancient microbial metabolic dynamics, caution needs to be exercised regarding isotope exchange during degradation and the mixing of multiple (microbial) sources after deposition (Sessions et al., 2004; Sessions, 2016; Häggi et al., 2021).

The soil microbial metabolism is dominated by heterotrophy across our three habitats. In peatland, meadow, and woodland, most $\varepsilon C_{FA/bulk}$ values are > -2‰ (Fig. 3b), indicating that the carbon isotopic discrimination during microbial assimilation is relatively small. Such small (negligible) fractionation is generally associated with heterotrophs, which directly utilize organic carbon and produce lipids that are only slightly depleted relative to the substrate (Blair et al., 1985; Hayes, 1993, 2001; Abraham et al., 1998; Pancost and Sinninghe Damsté, 2003; Cowie et al., 2009). Moreover, we observed many positive $\varepsilon C_{FA/bulk}$ values (Fig. 3b), suggesting that microorganisms in our soil habitats preferentially utilize substrates with higher $\delta^{13}C$ values compared to $\delta^{13}C_{bulk}$. These substrates could be carbohydrates, which typically have higher $\delta^{13}C$ values compared to other organic substrates (van Dongen et al., 2001;

563 Hobbie and Werner, 2004; Badeck et al., 2005). For example, van Dongen et al. (2002)
564 found that the $\delta^{13}C$ values of monosaccharides were ca. 2~10 ‰ more enriched (higher)
565 compared to $\delta^{13}C_{bulk}$ in a peat bog. Our results are consistent with the heterotrophic
566 ecology indicated by the $\delta^{13}C$ values of bacteria-derived C_{31} hopane in peatlands (Inglis
567 et al., 2019), suggesting that a wide range of hopane- and PLFAs-producing bacteria
568 and eucaryotic microbes in peatlands are preferentially using carbohydrates for their
569 anabolism.

570 The $\varepsilon H_{FA/water}$ values further support the dominance of heterotrophy across the three
571 habitats. Most $\varepsilon H_{FA/water}$ values are > -160 ‰ (Fig. 4b), falling in the lower part of the
572 range of heterotrophic bacterial $\varepsilon H_{FA/water}$ (-160 ‰ ~ +400‰) found in laboratory
573 cultures (e.g., Sessions et al., 2002; Zhang et al., 2009; Dirghangi and Pagani, 2013;
574 Fang et al., 2014; Heinzelmann et al., 2015a, b; Wijker et al., 2019). This indicates that
575 the hydrogen isotope fractionation of microbial fatty acids can reflect microbial
576 metabolism information that is consistent with that based on stable carbon isotopes,
577 perhaps providing mechanistic insight into the significant correlation between $\varepsilon C_{FA/bulk}$
578 and $\varepsilon H_{FA/water}$.

579 But we can potentially go further. Laboratory culture experiments have found that
580 heterotrophic microorganisms growing on TCA-cycle precursors and intermediates
581 (acetate, citrate, and succinate) produce fatty acids with $\varepsilon H_{FA/water} > 0$ and up to +400 ‰
582 (Zhang et al., 2009; Heinzelmann et al., 2015b; Osburn et al., 2016; Wijker et al., 2019).
583 In contrast, heterotrophs growing on sugars and using Embden-Meyerhof-Parnas
584 (EMP), pentose phosphate (PP), and Entner-Doudoroff (ED) pathways typically have

585 lower $\varepsilon H_{FA/water}$ values (-150 to 0 ‰) compared to those using TCA cycle substrates
586 (Zhang et al., 2009; Wijker et al., 2019). The positive $\varepsilon H_{FA/water}$ values (^2H-enriched
587 fatty acids) were suggested to be caused by $NADP^+$ reduction and dehydrogenase
588 reactions in the TCA cycle, which can lead to strong ^2H enrichment of NADPH (ref. to
589 Zhang et al., 2009). Thus, $\varepsilon H_{FA/water}$ values of fatty acids derived from normal TCA-
590 cycle substrates can be as high as +400 ‰. We did not find any fatty acids with a
591 $\varepsilon H_{FA/water}$ value > 0 or < -220 ‰ (Fig. 4b). Therefore, our hydrogen isotope data suggest
592 that the metabolic pathway of heterotrophs in our soils is dominated by carbohydrate –
593 likely cellulose-derived – rather than solely TCA-cycle substrates, consistent with their
594 positive $\varepsilon C_{FA/bulk}$ values.

595 The above inference is based on laboratory cultures of heterotrophic bacteria.
596 However, an alternative heterotrophic source for soil PLFAs is fungi, for which there
597 are no data on their lipid hydrogen isotope fractionation. The classic PLFA marker for
598 soil fungi is polyunsaturated 18:2ω6,9c (Frostegård and Bååth, 1996; Frostegård et al.,
599 2011). However, in our samples, the abundance of 18:2ω6,9c is low, accounting for
600 only 1.3 % of the total PLFAs. Quantitative PCR investigations have also found that
601 fungi gene abundance in peatlands is minor, only about 1.4 % of total prokaryotes (Lin
602 et al., 2012). The low fungal abundance could be related to the long-term waterlogged
603 conditions of the Dajiuhu basin, as many fungi are obligate aerobes (Clark et al., 2020).
604 Despite the low abundance, considering the possibility of different fractionations
605 between fungi and bacteria is important (Supplementary Material Text S2).

606 The correlation slope is consistent across different habitats and individual PLFA (Fig.
607 6). The linear regression slope of dual isotopic fractionation has been used to describe
608 the aerobic and anaerobic microbial degradation of aromatic hydrocarbons (Elsner et
609 al., 2007; Fischer et al., 2008; Vogt et al., 2008; Dorer et al., 2014; Musat et al., 2016).
610 Our results show that the slope for PLFAs in the peatland, meadow, and woodland soils
611 is similar, with values around 6.0 (Fig. 6f). There is also no significant difference
612 between the slopes of different individual PLFA (one-way ANOVA, $p > 0.05$), this again
613 points towards conservative microbial metabolism in natural peat and soil systems. Our
614 slopes appear to be lower than those derived from aerobic methanotrophy (in both
615 laboratory culture and the natural environment), which ranges from 7.3 to 10.5
616 (Feisthauer et al., 2011; Kawagucci et al., 2021). Despite the relatively large error in
617 our slope (Fig. 6f), these values do not differ significantly. To further assess whether
618 the dual isotope-derived correlation slope can be used as a potential indicator of
619 different microbial metabolisms, additional paired data is required.
620
621 4.3. Characteristics of carbon and hydrogen isotope fractionation of methanotrophy
622 Even though our dual carbon and hydrogen isotopic approach suggests heterotrophy
623 dominates the microbial metabolism in our soils, there are still key differences between
624 the three habitats. Compared with meadows and woodlands, the $\delta^{13}C$ and $\varepsilon C_{FA/bulk}$
625 values of PLFAs in peatlands are 2 ~ 10 ‰ lower (Fig. 3), especially the two
626 monounsaturated fatty acids, 16:1ω7c and 18:1ω7c, which have the largest $\varepsilon C_{FA/bulk}$
627 differences (avg. 5 ‰) between peatland and meadow/woodland (Fig. 3b). These are

628 the dominant fatty acids found in methanotrophic strains isolated from peatlands and
629 *Sphagnum* mosses (Dedysh et al., 2002, 2004; Bodelier et al., 2009; Dedysh, 2009; Kip
630 et al., 2011). In addition, stable isotope labeling ($^{13}CH_4$) experiments show that 16:1ω7c,
631 18:1ω7c, and 18:1ω9c are primary methanotrophic fatty acids in peatlands (Chen et al.,
632 2008; van Winden et al., 2010). High-throughput sequencing of the 16S rRNA gene has
633 revealed the existence of methanotrophs (mainly type II) in peat samples from our study
634 site (Xiang et al., 2023), and our preceding investigation also implies that the ^{13}C-
635 depletion of these monounsaturated PLFAs is associated with decreased methane
636 emission fluxes (Zhang et al., 2022b). Therefore, the larger carbon isotopic offset (lower
637 $\varepsilon C_{FA/bulk}$ values) of 16:1ω7c and 18:1ω7c we observe in the peatland samples (Fig. 3b)
638 is likely due to these compounds being partly derived from methanotrophs, reflecting
639 both a more ^{13}C-depleted substrate as well as a larger carbon isotopic fractionation than
640 occurs during heterotrophy (Summons et al., 1994; Jahnke et al., 1999; Cifuentes and
641 Salata, 2001; Mills et al., 2010; Simkus et al., 2016).

642 However, the hydrogen isotopic offset ($\varepsilon H_{FA/water}$) of the same PLFAs does not differ
643 significantly (one-way ANOVA, $p > 0.05$) from those of putative heterotrophic
644 microbes in meadow/woodland environments. This suggests that the putative
645 methanotrophic PLFAs may not necessarily have large hydrogen isotope fractionations.
646 Interestingly, culture experiments show that methane-oxidizing bacteria have $\varepsilon H_{FA/water}$
647 values between +37 and -161 ‰ (Sessions et al., 1999, 2002). This value falls within
648 the heterotrophic $\varepsilon H_{FA/water}$ range (-160 to +400 ‰) (e.g., Zhang et al., 2009;

649 Heinzelmann et al., 2015a; Wijker et al., 2019). Thus, $\varepsilon H_{FA/water}$ seems unable to clearly
650 distinguish methanotrophy from heterotrophy (Sessions et al., 2002).

651 Therefore, methanotroph fatty acids have larger carbon isotope fractionations (low
652 $\varepsilon C_{FA/bulk}$ values) but limited hydrogen isotope fractionation (relatively high $\varepsilon H_{FA/water}$
653 values) in laboratory and natural environments. We refer to this as the decoupling
654 between their $\varepsilon C_{FA/bulk}$ and $\varepsilon H_{FA/water}$, as they differ from other PLFAs that have coupled
655 high (low) $\varepsilon C_{FA/bulk}$ and high (low) $\varepsilon H_{FA/water}$ values. The lack of a strong relationship
656 between the $\delta^{13}C$ and $\delta^{2}H$ values for 18:1ω7c and 18:1ω9c confirms this decoupling
657 (Fig. 6c). Since the study site is mainly inhabited by type II methanotrophs (mainly
658 producing C_{18} monounsaturated PLFAs), the partial methanotrophic origin of 16:1ω7c
659 need to be treated with caution. Thus, the significant correlation between $\delta^{13}C$ and $\delta^{2}H$
660 of 16:1ω7c may be related to its primarily heterotrophic origin. Several other PLFAs
661 that exhibit a decoupling of their $\varepsilon C_{FA/bulk}$ and $\varepsilon H_{FA/water}$, such as 10Me16:0 and cy19:0
662 (Fig. 5b and Fig. 6c), could also have either partial methanotrophic origins or unique
663 biosynthetic pathways. However, these PLFAs have fewer diagnostic origins, making
664 the interpretation of their decoupling more challenging. Below, we explore the possible
665 reasons for the decoupling of carbon and hydrogen isotopes in certain PLFAs.

666 For methanotrophic origins, although methanotrophs use methane as a carbon source,
667 the hydrogen for methanotrophic lipid biosynthesis does not come directly from
668 methane. Instead, it comes from growth water as well as water derived from methane
669 oxidation (Sessions et al., 2002). This water can contribute to the NADPH pool through
670 isotopic exchange, where it serves as a hydrogen source during lipid biosynthesis

671 (Zhang et al., 2009). Therefore, the $\varepsilon H_{FA/water}$ of methanotrophic PLFAs could be
672 determined by the NADPH metabolism during methanotrophy. This occurs mainly in
673 two pathways: the ribulose monophosphate pathway (RuMP) and the serine pathway
674 (e.g., Hanson and Hanson,1996; Bodelier et al., 2009). Importantly, in the RuMP,
675 NADPH metabolism is related to the ED and EMP pathways via pyruvate formation,
676 and in the serine pathway, it is related to the ethylmalonyl-CoA (EMC) pathway for
677 glyoxylate production (Chistoserdova et al., 2009; Kalyuzhnaya et al., 2013). The ED,
678 EMP, and EMC pathways are also used by aerobic heterotrophic bacteria in glucose
679 catabolism (Alber et al., 2010; Wijker et al., 2019). Therefore, methanotrophs may
680 undergo similar NADPH metabolism as heterotrophs and have relatively high $\varepsilon H_{FA/water}$
681 values (+37 to -161 ‰, Sessions et al., 1999, 2002). In contrast to hydrogen, the carbon
682 of methanotrophic lipids comes from ^{13}C-depleted methane, and the carbon isotope
683 fractionation mainly occurs during the catalytic reaction of methane monooxygenase.
684 This combination results in the decoupled high $\varepsilon H_{FA/water}$ and low $\varepsilon C_{FA/bulk}$ values of
685 methanotrophic lipids.

686 Our results verify the expected methanotrophy-related carbon but not hydrogen
687 depletion in natural soils, providing specific insight into the combination of PLFA δ^2H
688 and $\delta^{13}C$ values. In particular, the decoupling of δ^2H and $\delta^{13}C$ provides a dual isotopic
689 approach for more robust identification of methanotrophy. For example, if a low
690 $\varepsilon C_{FA/bulk}$ ($\delta^{13}C$) value cannot distinguish methanotrophy and autotrophy, a relatively
691 high $\varepsilon H_{FA/water}$ (δ^2H) value provides evidence for the former and a low value for the
692 latter. The pairing of carbon and hydrogen isotopes in methanotrophic lipids needs to

693 further studied in different natural environments, as different sources of hydrogen can
694 be used in the biosynthesis of these lipids. For example, in lake and pond water columns
695 with high methane oxidation efficiency, the hydrogen used for the biosynthesis of
696 methanotroph-associated lipids can mainly come from the ^{2}H-depleted products of
697 methane oxidation, resulting in significantly low $\delta^{2}H$ values of moss-derived C_{21} and
698 C_{23} *n*-alkanes (McFarlin et al., 2023). Thus, it is essential to consider the source of
699 hydrogen isotopes used for methanotrophic lipid biosynthesis when connecting lipid
700 isotopic signals with methanotrophy.
701
702 4.4. Impacts of lipid biosynthesis pathway and environmental parameters
703 The relationship between the carbon and hydrogen isotopic composition of PLFAs is
704 also embedded in their lipid biosynthetic pathways. For example, a positive correlation
705 between $\varepsilon C_{lipid/bulk}$ and $\varepsilon H_{lipid/water}$ has been found in fatty acids and *n*-alkanes from
706 terrestrial and aquatic plants (Chikaraishi and Naraoka, 2003; Chikaraishi et al., 2004).
707 In contrast, phytol and sterols in terrestrial and aquatic plants have a negative
708 correlation between $\varepsilon C_{lipid/bulk}$ and $\varepsilon H_{lipid/water}$ (Chikaraishi et al., 2004). Phytol and sterol
709 are isoprenoid lipids synthesized through 1-deoxy-D-xylulose-5-phosphate (DOXP) /2-
710 methylerythroyl-4-phosphate (MEP) and mevalonic acid (MVA) pathways, while fatty
711 acids are derived from acetogenic pathways (Lichtenthaler, 1999; Schmidt et al., 2003;
712 Chikaraishi et al., 2004; Zhang and Sachs, 2007; Sachse et al., 2012).
713 Moreover, our results show that the a15:0 and a17:0 lipids have an average $\varepsilon H_{FA/water}$
714 value < -160 ‰, with some values as low as -200 ‰ (Fig. 4b). Previous culture

715 experiments found that such anteiso fatty acids from sulfate-reducing bacteria are more
716 depleted in ^{2}H and that these lipids have lower $\varepsilon H_{FA/water}$ values than their straight-chain
717 saturated counterparts (Leavitt et al., 2016, 2017). This depletion could be related to the
718 biosynthetic pathway of anteiso fatty acids. Unlike straight-chain fatty acids, which use
719 acetyl-CoA as the primer, anteiso fatty acids use 2-methylbutyryl-CoA from isoleucine
720 as the primer for carbon chain extension (Kaneda, 1991). Thus, the precursor isoleucine
721 with low $\delta^{2}H$ values appears to lead to the ^{2}H-depletion in anteiso fatty acids (Leavitt
722 et al., 2016). Indeed, our results show that the $\delta^{2}H$ value of a15:0 is significantly (one-
723 way ANOVA, $p < 0.01$) lower than the other PLFAs (Fig. 6b). Our work is the first
724 observation of this biosynthetic profile in nature, and it could be a useful tool for
725 assessing the fidelity of PLFA $\delta^{2}H$ distributions in future studies.

726 Our results also illustrate the potential controls that soil environmental parameters
727 have on the carbon and hydrogen isotopic composition of PLFAs. Soil water content
728 (SWC) and the total organic carbon content (TOC) are positively correlated with each
729 other, and both are negatively correlated with $\delta^{13}C$ ($\varepsilon C_{FA/bulk}$) (Fig. 5). This correlation
730 is nearly entirely dictated by the inclusion of a peatland site that is water-saturated,
731 anaerobic, and organic-rich (Table 1; Reddy et al., 2022; Zhang et al., 2022b). The
732 negative relationship with the putative methanotroph-derived PLFA $\varepsilon C_{FA/bulk}$ is
733 expected, given the control of SWC on methanogenesis (e.g., Praeg et al., 2014).
734 However, almost all PLFAs have lower carbon isotopic compositions in the peatland
735 (Fig. 3). This could reflect the distribution of methane-derived carbon through the wider
736 bacterial community, which can be achieved through direct predation, and absorption

737 of metabolites and necromass of methanotrophs by heterotrophs (Deines et al., 2007;
738 Maxfield et al., 2012). Consistent with that, a simple mass balance, assuming that
739 methanotroph PLFA $\delta^{13}C$ values are ~ -64 ‰ and non-methanotroph PLFAs are -
740 26.5 ‰, yields a 6.6 % methanotroph contribution to the total PLFA pool for the
741 peatland and a negligible contribution for the woodland and meadow (Supplementary
742 Material Text S3). Alternatively, or additionally, the ^{13}C depletion of all PLFAs in
743 peatlands may be more consistent with all changes in microbial fractionation
744 (Supplementary Material Text S4). Moreover, the concentration of NO_3^--N and NH_4^+-
745 N may also alter the isotope signals of PLFAs by impacting the metabolic activity of
746 nitrogen-cycling microorganisms (Supplementary Material Text S4).

747 The relationship between $\varepsilon H_{FA/water}$ and SWC is limited to several iso- and anteiso-
748 branched PLFAs (Fig. 5). Previous studies found that under anaerobic conditions,
749 microorganisms exhibit greater hydrogen isotope fractionation between their lipids and
750 source water (e.g., Valentine et al., 2004; Campbell et al., 2009; Li et al., 2009; Zhang
751 et al., 2009; Dawson et al., 2015; Heinzelmann et al., 2015b); however, these larger
752 fractionations are generally associated with photoautotrophy and chemoautotrophy.
753 Similar $\varepsilon H_{FA/water}$ values of microbial fatty acids between anaerobic and aerobic
754 conditions were reported in several culture experiments (e.g., Leavitt et al., 2016;
755 Osburn et al., 2016). Thus, the control of redox condition on microbial lipid hydrogen
756 isotope fractionation seems more complex than that of stable carbon isotopes.

757

758 **5. CONCLUSIONS**

This study investigated the stable carbon and hydrogen isotopic composition of microbial PLFAs in natural soil environments. Together with measurements of environmental and bulk geochemical parameters such as soil water content, total organic carbon content, nutrients, $\delta^{13}C_{bulk}$, and $\delta^{2}H_{water}$, etc., we explored the nature and possible controls on $\varepsilon C_{FA/bulk}$ and $\varepsilon H_{FA/water}$ of PLFAs in peatlands, meadows, and woodlands. We used this data to evaluate the relationship between carbon and hydrogen isotopes of PLFAs and discuss the implications. The main findings are as follows:

(1) The carbon and hydrogen isotope composition and offset of PLFAs show a significant positive correlation, supporting the dominant control of central metabolic pathways on both carbon and hydrogen isotopic fractionation of microbial fatty acids. The narrow range of $\varepsilon C_{FA/bulk}$ and $\varepsilon H_{FA/water}$ values and the consistency of dual-isotopic-derived correlation slope across all three habitats reflect the conservative and consistent nature of soil microbial metabolism, which is dominated by carbohydrate-consuming heterotrophy with just a bit of methanotrophy.

(2) The monounsaturated PLFAs, related to methanotrophs, in peatlands have lower $\varepsilon C_{FA/bulk}$ but not $\varepsilon H_{FA/water}$ values, revealing that methanotrophic-derived carbon isotope depletion that need not also impact their hydrogen isotopic composition in natural environments. This decoupling of $\delta^{2}H$ and $\delta^{13}C$ provides a dual-isotope method to identify methanotrophy. Our work is also the first observation of biosynthetic pathways affecting the $\delta^{2}H$ distribution of anteiso fatty acids in natural soils.

We demonstrate the potential consistency of dual isotopic methods in reflecting microbial metabolic activity in natural soil environments. The dual isotopic

fractionation pattern can not only provide more information and act as a cross-check on microbial metabolism, but also build a framework for evaluating soil microbial community metabolic perturbations. In the future, the diagnostic dual isotope fractionation patterns of microbial lipids may become a powerful tool for exploring significant shifts in microbial activity in various modern environments and the geological record. We hope future studies will further constrain the carbon and hydrogen isotope fractionation in laboratory cultures and natural environments to characterize these relationships in different metabolic pathways, leading to new approaches for reconstructing past variations in microbial metabolic activity.

ACKNOWLEDGEMENTS

This work was supported by the National Natural Science Foundation of China (U20A2094, 91951208), the 111 project from the Ministry of Education of China (BP0820004), and the China Postdoctoral Science Foundation (2022M722937). Dr. Ruicheng Wang, Bingyan Zhao, Yang Yang, Xiaofang Yu, Yuhang Wang, Chaoyang Yan, Xin Yang, Ting Yang, and Fanfan Yang are thanked for their help in the field and the laboratory analysis. B.D.A.N. acknowledges funding through a Royal Society Tata University Research Fellowship and R.D.P acknowledges funding from UK Research and Innovation (UKRI) under the UK government's Horizon Europe funding guarantee [CERES EP/X023214/1]. We especially thank the reviewers, Alex Sessions, Jamie McFarlin, and two anonymous reviewers, whose constructive comments substantially improved this manuscript.

Data Availability

Data are available through Mendeley Data at http://dx.doi.org/10.17632/pwhtt9jtdn.1.

Appendix A. Supplementary Material

This Supplementary Material includes Supplementary Figures S1-S2, Supplementary Texts S1-S4, and related references. Fig. S1, air temperature and precipitation in the Dajiuhu basin; Fig. S2, recalculated $\varepsilon H_{FA/water}$ using the simulated long-term average δ^2H of soil water; Text S1, the root reason for the correlation between the carbon and hydrogen isotopes of microbial PLFAs; Text S2, fungal hydrogen isotope fractionation; Text S3, quantitative estimation of methane-derived carbon; Text S4, impacts of environmental parameters.

REFERENCES

Abraham W. R., Hesse C. and Pelz O. (1998) Ratios of carbon isotopes in microbial lipids as an indicator of substrate usage. *Appl. Environ. Microbiol.* **64**, 4202–4209.

Alber B. E. (2011) Biotechnological potential of the ethylmalonyl-CoA pathway. *Appl. Microbiol. Biotechnol* **89**, 17–25.

Allan E., Douglas P. M., de Vernal A., Gélinas Y. and Mucci A. O. (2023) Palmitic acid is not a proper salinity proxy in Baffin Bay and the Labrador Sea but reflects the variability in organic matter sources modulated by sea ice coverage. *Geochem. Geophy. Geosy.* **24**, e2022GC010837.

825 Andersen R., Chapman S. J. and Artz, R. R. E. (2013) Microbial communities in natural
826 and disturbed peatlands: a review. *Soil Biol. Biochem.* **57**, 979–994.
827 Badeck F. W., Tcherkez G., Nogues S., Piel C. and Ghashghaie J. (2005) Post-
828 photosynthetic fractionation of stable carbon isotopes between plant organs-a
829 widespread phenomenon. *Rapid Commun. Mass Spectrom.* **19**, 1381–1391.
830 Bardgett R. D., Freeman C., Ostle N. J. (2008) Microbial contributions to climate
831 change through carbon cycle feedbacks. *ISME J.* **2**, 805–814.
832 Billings S. A. and Ziegler S. E. (2008) Altered patterns of soil carbon substrate usage
833 and heterotrophic respiration in a pine forest with elevated CO_2 and N fertilization.
834 *Glob. Chang Biol.* **14**, 1025–1036.
835 Blair N., Leu A., Munoz E., Olsen J., Kwong E. and des Marais D. (1985) Carbon
836 isotopic fractionation in heterotrophic microbial metabolism. *Appl. Environ.*
837 *Microbiol.* **50**, 996–1001.
838 Blewett J., Elling F. J., Naafs B. D. A., Kattein L., Evans T. W., Lauretano V., Gallego-
839 Sala A.V., Pancost R. D. and Pearson A. (2022) Metabolic and ecological controls
840 on the stable carbon isotopic composition of archaeal (isoGDGT and BDGT) and
841 bacterial (brGDGT) lipids in wetlands and lignites. *Geochim. Cosmochim. Acta* **320**,
842 1–25.
843 Bligh E. G. and Dyer W. J. (1959) A rapid method of total lipid extraction and
844 purification. *Can. J. Biochem. Phys.* **37**, 911–917.
845 Bodelier P. L., Gillisen M. J. B., Hordijk K., Sinninghe Damsté J. S., Rijpstra W. I. C.,
846 Geenevasen J. A. and Dunfield P. F. (2009) A reanalysis of phospholipid fatty acids

847 as ecological biomarkers for methanotrophic bacteria. *ISME J.* **3**, 606–617.
848 Boschker H. T. S., De Brouwer J. F. C. and Cappenberg T. E. (1999) The contribution
849 of macrophyte-derived organic matter to microbial biomass in salt-marsh sediments:
850 Stable carbon isotope analysis of microbial biomarkers. *Limnol. Oceanogr.* **44**, 309–
851 319.
852 Boschker H. T. S., and Middelburg J. J. (2002) Stable isotopes and biomarkers in
853 microbial ecology. *FEMS Microbiol. Ecol.* **40**, 85–95.
854 Bossio D. A. and Scow K. M. (1998) Impacts of carbon and flooding on soil microbial
855 communities: Phospholipid fatty acid profiles and substrate utilization patterns.
856 *Microb. Ecol.* **35**, 265–278.
857 Bowen G. J., Wassenaar L. I. and Hobson K. A. (2005) Global application of stable
858 hydrogen and oxygen isotopes to wildlife forensics. *Oecologia* **143**, 337–348.
859 Bowen G. J. (2023) The Online Isotopes in Precipitation Calculator, version 3.1.
860 http://www.waterisotopes.org.
861 Brady A. L., Slater G. F., Omelon C. R., Southam G., Druschel G., Andersen D. T.,
862 Hawes I., Laval B. and Lim D. S. S. (2010) Photosynthetic isotope biosignatures in
863 laminated micro-stromatolitic and non-laminated nodules associated with modern,
864 freshwater microbialites in Pavilion Lake, BC. *Chem. Geol.* **274**, 56–67.
865 Brady A. L., Laval B., Lim D. S. S. and Slater G. F. (2014) Autotrophic and
866 heterotrophic associated biosignatures in modern freshwater microbialites over
867 seasonal and spatial gradients. *Org. Geochem.* **67**, 8–18.
868 Brady A. L., Goordial J., Sun H. J., Whyte L. G. and Slater G. F. (2018) Variability in

carbon uptake and (re) cycling in Antarctic cryptoendolithic microbial ecosystems demonstrated through radiocarbon analysis of organic biomarkers. *Geobiology* **16**, 62–79.

Burke R. A., Molina M., Cox J. E., Osher L. J. and Piccolo M. C. (2003) Stable carbon isotope ratio and composition of microbial fatty acids in tropical soils. *J. Environ. Qual.* **32**, 198–206.

Campbell B. J., Li C., Sessions A. L. and Valentine D. L. (2009) Hydrogen isotopic fractionation in lipid biosynthesis by H_2-consuming *Desulfobacterium autotrophicum*. *Geochim. Cosmochim. Acta* **73**, 2744–2757.

Campbell B. J., Sessions A. L., Fox D. N., Paul B. G., Qin Q., Kellermann M. Y. and Valentine D. L. (2017) Minimal influence of [NiFe] hydrogenase on hydrogen isotope fractionation in H_2-oxidizing *Cupriavidus necator*. *Front. Microbiol.* **8**, 1886.

Caro T. A., McFarlin J., Jech S., Fierer N. and Kopf S. (2023) Hydrogen stable isotope probing of lipids demonstrates slow rates of microbial growth in soil. *Proc. Natl. Acad. Sci. U.S.A.* **120(16)**, e2211625120.

Chen Y., Dumont M. G., McNamara N. P., Chamberlain P. M., Bodrossy L., Stralis-Pavese N. and Murrell J. C. (2008) Diversity of the active methanotrophic community in acidic peatlands as assessed by mRNA and SIP-PLFA analyses. *Environ. Microbiol.* **10**, 446–459.

Chen X., Liu X., Wei Y. and Huang Y. (2019) Production of long-chain *n*-alkyl lipids by heterotrophic microbes: new evidence from Antarctic lakes. *Org. Geochem.* **138**,

891 103909.

892 Chen X., Liu X., Jia H., Jin J., Kong W. and Huang Y. (2021) Inverse hydrogen isotope
893 fractionation indicates heterotrophic microbial production of long-chain *n*-alkyl
894 lipids in desolate Antarctic ponds. *Geobiology* **19**, 394–404.

895 Chikaraishi Y. and Naraoka H. (2003) Compound-specific δD–δ^{13}C analyses of *n*-
896 alkanes extracted from terrestrial and aquatic plants. *Phytochemistry* **63**, 361–371.

897 Chikaraishi Y., Naraoka H. and Poulson S. R. (2004) Hydrogen and carbon isotopic
898 fractionations of lipid biosynthesis among terrestrial (C_3, C_4 and CAM) and aquatic
899 plants. *Phytochemistry* **65**, 1369–1381.

900 Chistoserdova L., Kalyuzhnaya M. G. and Lidstrom M. E. (2009) The expanding world
901 of methylotrophic metabolism. *Annu. Rev. Microbiol.* **63**, 477.

902 Cifuentes L. A. and Salata G. G. (2001) Significance of carbon isotope discrimination
903 between bulk carbon and extracted phospholipid fatty acids in selected terrestrial
904 and marine environments. *Org. Geochem.* **32**, 613–621.

905 Clark M. A., Douglas M. and Choi J. (2020) Biology 2e. OpenStax, Rice University,
906 Houston. https://openstax.org.

907 Coplen T. B. (2011) Guidelines and recommended terms for expression of stable-
908 isotope-ratio and gas-ratio measurement results. *Rapid Commun. Mass Spectrom.*
909 **25**, 2538–2560.

910 Cowie B. R., Slater G. F., Bernier L. and Warren L. A. (2009) Carbon isotope
911 fractionation in phospholipid fatty acid biomarkers of bacteria and fungi native to
912 an acid mine drainage lake. *Org. Geochem.* **40**, 956–962.

913 Dawson K. S., Osburn M. R., Sessions A. L. and Orphan V. J. (2015) Metabolic
914 associations with archaea drive shifts in hydrogen isotope fractionation in sulfate-
915 reducing bacterial lipids in cocultures and methane seeps. *Geobiology* **13**, 462–477.
916 Dedysh S. N., Khmelenina V. N., Suzina N. E., Trotsenko Y. A., Semrau J. D., Liesack
917 W. and Tiedje J. M. (2002) *Methylocapsa acidiphila* gen. nov., sp. nov., a novel
918 methane-oxidizing and dinitrogen-fixing acidophilic bacterium from *Sphagnum*
919 bog. *Int. J. Syst. Evol. Microbiol.* **52**, 251–261.
920 Dedysh S. N., Berestovskaya Y. Y., Vasylieva L. V., Belova S. E., Khmelenina V. N.,
921 Suzina N. E., Trotsenko Y. A., Liesack W. and Zavarzin G. A. (2004) *Methylocella*
922 *tundrae* sp. nov., a novel methanotrophic bacterium from acidic tundra peatlands.
923 *Int. J. Syst. Evol. Microbiol.* **54**, 151–156.
924 Dedysh S. N. (2009) Exploring methanotroph diversity in acidic northern wetlands:
925 Molecular and cultivation-based studies. *Microbiology* **78**, 655–669.
926 Dickson L., Bull I. D., Gates P. J. and Evershed R. P. (2009) A simple modification of
927 a silicic acid lipid fractionation protocol to eliminate free fatty acids from glycolipid
928 and phospholipid fractions. *J. Microbiol. Methods* **78**, 249–254.
929 Dippold M. A. and Kuzyakov Y. (2016) Direct incorporation of fatty acids into
930 microbial phospholipids in soils: position-specific labeling tells the story. *Geochim.*
931 *Cosmochim. Acta* **174**, 211–221.
932 Dirghangi S. S. and Pagani M. (2013) Hydrogen isotope fractionation during lipid
933 biosynthesis by Tetrahymena thermophila. *Org. Geochem.* **64**, 105–111.
934 Dorer C., Vogt C., Kleinsteuber S., Stams A. J. and Richnow H. H. (2014) Compound-

935 specific isotope analysis as a tool to characterize biodegradation of ethylbenzene.
936 *Environ. Sci. Technol.* **48**, 9122–9132.
937 Dowling N. J. E., Widdel F. and White D. C. (1986) Phospholipid ester-linked fatty acid
938 biomarkers of acetate-oxidizing sulphatereducers and other sulphide-forming
939 bacteria. *J. Gen. Microbiol.* **132**, 1815–1825.
940 Elsner M., McKelvie J., Lacrampe Couloume G. and Sherwood Lollar B. (2007) Insight
941 into methyl tert-butyl ether (MTBE) stable isotope fractionation from abiotic
942 reference experiments. *Environ. Sci. Technol.* **41**, 5693–5700.
943 Elvert M., Pohlman J. W., Becker K. W., Gaglioti B., Hinrichs K. U. and Wooller M. J.
944 (2016) Methane turnover and environmental change from Holocene lipid biomarker
945 records in a thermokarst lake in Arctic Alaska. *Holocene* **26**, 1766–1777.
946 Evershed R. P., Bull I. D., Corr L. T., Crossman Z. M., van Dongen B. E., Evans C. J.,
947 Jim S., Mottram H. R., Mukherjee A. J. and Pancost R. D. (2008) Compound-
948 specific stable isotope analysis in ecology and paleoecology. In *Stable Isotopes in*
949 *Ecology and Environmental Science* (ed. R. Michener and K. Lajtha), pp. 480–540.
950 Blackwell Publishing Ltd, Oxford.
951 Fang J., Chan O., Joeckel R. M., Huang Y., Wang Y., Bazylinski D. A., Moorman T. B.
952 and Clement B. J. A. (2006) Biomarker analysis of microbial diversity in sediments
953 of a saline groundwater seep of Salt Basin, Nebraska. *Org. Geochem.* **37**, 912–931.
954 Fang J., Li C., Zhang L., Davis T., Kato C. and Bartlett D. H. (2014) Hydrogen isotope
955 fractionation in lipid biosynthesis by the piezophilic bacterium Moritella japonica
956 DSK1. *Chem. Geol.* **367**, 34–38.

957 Feakins S. J., Wu M. S., Ponton C., Galy V. and West A. J. (2018) Dual isotope evidence
958 for sedimentary integration of plant wax biomarkers across an Andes-Amazon
959 elevation transect. *Geochim. Cosmochim. Acta* **242**, 64–81.
960 Feisthauer S., Vogt C., Modrzynski J., Szlenkier M., Krüger M., Siegert M. and
961 Richnow H. H. (2011) Different types of methane monooxygenases produce similar
962 carbon and hydrogen isotope fractionation patterns during methane oxidation.
963 *Geochim. Cosmochim. Acta* **75**, 1173–1184.
964 Fenner N., Freeman C. and Reynolds B. (2005) Observations of a seasonally shifting
965 thermal optimum in peatland carbon-cycling processes; implications for the global
966 carbon cycle and soil enzyme methodologies. *Soil Biol. Biochem.* **37**(10), 1814–
967 1821.
968 Fischer A., Herklotz I., Herrmann S., Thullner M., Weelink S. A., Stams A. J.,
969 Schlomann M., Richnow H. H. and Vogt C. (2008) Combined carbon and hydrogen
970 isotope fractionation investigations for elucidating benzene biodegradation
971 pathways. *Environ. Sci. Technol.* **42**, 4356–4363.
972 Frostegård A. and Bååth E. (1996) The use of phospholipid fatty acid analysis to
973 estimate bacterial and fungal biomass in soil. *Biol. Fertil. Soils* **22**, 59–65.
974 Frostegård A., Tunlid A. and Bååth E. (2011) Use and misuse of PLFA measurements
975 in soils. *Soil Biol. Biochem.* **43**, 1621–1625.
976 Häggi C., Pätzold J., Bouillon S. and Schefuβ E. (2021) Impact of selective degradation
977 on molecular isotope compositions in oxic and anoxic marine sediments. *Org.*
978 *Geochem.* **153**, 104192.

979 Hanson R. S. and Hanson T. E. (1996) Methanotrophic bacteria. *Microbiol. Rev.* **60**,
980 439–471.
981 Hayes J. M., Freeman K. H., Popp B. N. and Hoham C. H. (1990) Compound-specific
982 isotopic analyses: a novel tool for reconstruction of ancient biogeochemical
983 processes. *Org. Geochem.* **16**, 1115–1128.
984 Hayes J. M. (1993) Factors controlling ^{13}C contents of sedimentary organic compounds:
985 Principles and evidence. *Mar. Geol.* **113**, 111–125.
986 Hayes J. M. (2001) Fractionation of carbon and hydrogen isotopes in biosynthetic
987 processes. *Rev. Mineral. Geochem.* **43**, 225–277.
988 He D., Ladd S. N., Park J., Sachs J. P., Simoneit B. R., Smoak J. M. and Jaffé R. (2022)
989 Carbon and hydrogen isotopes of taraxerol in mangrove leaves and sediment cores:
990 Implications for paleo-reconstructions. *Geochim. Cosmochim. Acta* **324**, 262–279.
991 Heinzelmann S. M., Chivall D., M'Boule D., Sinke-Schoen D., Villanueva L.,
992 Sinninghe Damsté J. S., Schouten S. and van der Meer M. T. J. (2015a) Comparison
993 of the effect of salinity on the D/H ratio of fatty acids of heterotrophic and
994 photoautotrophic microorganisms. *FEMS Microbiol. Lett.* **362**, fnv065.
995 Heinzelmann S. M., Villanueva L., Sinke-Schoen D., Sinninghe Damsté J. S., Schouten
996 S. and van der Meer, M. T. J. (2015b) Impact of metabolism and growth phase on
997 the hydrogen isotopic composition of microbial fatty acids. *Front. Microbiol.* **6**, 408.
998 Heinzelmann S. M., Bale N. J., Villanueva L., Sinke-Schoen D., Philippart C. J. M.,
999 Sinninghe Damsté J. S., Schouten S. and van der Meer, M. T. J. (2016) Seasonal
1000 changes in the D/H ratio of fatty acids of pelagic microorganisms in the coastal

North Sea. *Biogeosciences* **13**, 5527–5539.

Heinzelmann S. M., Villanueva L., Lipsewers Y. A., Sinke-Schoen D., Sinninghe Damsté J. S., Schouten S. and van der Meer, M. T. J. (2018) Assessing the metabolism of sedimentary microbial communities using the hydrogen isotopic composition of fatty acids. *Org. Geochem.* **124**, 123–132.

Hill G. T., Mitkowski N. A., Aldrich-Wolfe L., Emele L. R., Jurkonie D. D., Ficke A., Maldonado-Ramirez S., Lynch S. T. and Nelson E. B. (2000) Methods for assessing the composition and diversity of soil microbial communities. *Appl. Soil Ecol.* **15**, 25–36.

Hobbie A. E. and Werner R. A. (2004) Intramolecular, compound-specific, and bulk carbon isotope patterns in C_3 and C_4 plants: a review and synthesis. *New Phytol.* **161**, 371–385.

Horita J. and Wesolowski D. J. (1994). Liquid-vapor fractionation of oxygen and hydrogen isotopes of water from the freezing to the critical temperature. *Geochim. Cosmochim. Acta* **58**, 3425–3437.

Huang X., Pancost R. D., Xue J., Gu Y., Evershed R. P. and Xie S. (2018) Response of carbon cycle to drier conditions in the mid-Holocene in central China. *Nat. Commun.* **9**, 1369.

Huang X. and Meyers P. A. (2019) Assessing paleohydrologic controls on the hydrogen isotope compositions of leaf wax *n*-alkanes in Chinese peat deposits. *Palaeogeogr. Palaeoclimatol. Palaeoecol.* **516**, 354–363.

Huang Y., Wang Y., Alexandre M. R., Lee T., Rose-Petruck C., Fuller M. and Pizzarello

1023 S. (2005) Molecular and compound-specific isotopic characterization of
1024 monocarboxylic acids in carbonaceous meteorites. *Geochim. Cosmochim. Acta* **69**,
1025 1073–1084.
1026 IAEA/WMO (2023). Global Network of Isotopes in Precipitation. The GNIP Database.
1027 Accessible at: https://nucleus.iaea.org/wiser.
1028 Inglis G. N., Naafs B. D. A., Zheng Y., Schellekens J. and Pancost R. D. (2019) $\delta^{13}C$
1029 values of bacterial hopanoids and leaf waxes as tracers for methanotrophy in
1030 peatlands. *Geochim. Cosmochim. Acta* **260**, 244–256.
1031 Jaatinen K., Fritze H., Laine J. and Laiho R. (2007) Effects of short- and long-term
1032 water-level drawdown on the populations and activity of aerobic decomposers in a
1033 boreal peatland. *Glob. Chang Biol.* **13**, 491–510.
1034 Jahnke L. L., Summons R. E., Hope J. M. and des Marais D. J. (1999) Carbon isotopic
1035 fractionation in lipids from methanotrophic bacteria II: The effects of physiology
1036 and environmental parameters on the biosynthesis and isotopic signatures of
1037 biomarkers. *Geochim. Cosmochim. Acta* **63**, 79–93.
1038 Jahnke L. L., Eder W., Huber R., Hope J. M., Hinrichs K. U., Hayes J. M., des Marais
1039 D. J., Cady S. L. and Summons R. E. (2001) Signature lipids and stable carbon
1040 isotope analyses of octopus spring hyperthermophilic communities compared with
1041 those of aquificales representatives. *Appl. Environ. Microbiol.* **67**, 5179–5189.
1042 Jansson J. K. and Hofmockel K. S. (2020) Soil microbiomes and climate change. *Nat.*
1043 *Rev. Microbiol.* **18**, 35–46.
1044 Jensen N. J. and Gross M. L. (1987) Mass spectrometry methods for structural

1045 determination and analysis of fatty acids. *Mass Spectrom. Rev.* **6**, 497–536.
1046 Jones A. A., Sessions A. L., Campbell B. J., Li C. and Valentine D. L. (2008) D/H ratios
1047 of fatty acids from marine particulate organic matter in the California Borderland
1048 Basins. *Org. Geochem.* **39**, 485–500.
1049 Kaiser C., Frank A., Wild B., Koranda M. and Richter A. (2010) Negligible contribution
1050 from roots to soil-borne phospholipid fatty acid fungal biomarkers 18:2ω6,9 and
1051 18:1ω9. *Soil Biol. Biochem.* **42**, 1650–1652.
1052 Kalyuzhnaya M. G., Yang S., Rozova O. N., Smalley N. E., Clubb J., Lamb A., Nagana
1053 Gowda G. A., Raftery D., Fu Y., Bringel F., Vuilleumier S., Beck D. A. C., Trotsenko
1054 Y. A., Khmelenina V. N. and Lidstrom M. E. (2013) Highly efficient methane
1055 biocatalysis revealed in a methanotrophic bacterium. *Nat. Commun.* **4**, 1–7.
1056 Kaneda T. (1991) Iso- and anteiso-fatty acids in bacteria: biosynthesis, function, and
1057 taxonomic significance. *Microbiol. Rev.* **55**, 288–302.
1058 Kawagucci S., Matsui Y., Makabe A., Fukuba T., Onishi Y., Nunoura T. and Yokokawa
1059 T. (2021) Hydrogen and carbon isotope fractionation factors of aerobic methane
1060 oxidation in deep-sea water. *Biogeosciences* **18**, 5351–5362.
1061 Kindler R., Miltner A., Thullner M., Richnow H. H. and Kästner M. (2009) Fate of
1062 bacterial biomass derived fatty acids in soil and their contribution to soil organic
1063 matter. *Org. Geochem.* **40**, 29–37.
1064 Kip N., Ouyang W., van Winden J., Raghoebarsing A., van Niftrik L., Pol A., Pan Y.,
1065 Bodrossy L., van Donselaar E. G., Reichart G.-J., Jetten M. S. M., Sinninghe
1066 Damsté J. S. and Op den Camp (2011) Detection, isolation, and characterization of

1067 acidophilic methanotrophs from *Sphagnum* mosses. *Appl. Environ. Microbiol.* **77**,
1068 5643–5654.
1069 Ladd S. N., Dubois N. and Schubert C. J. (2017) Interplay of community dynamics,
1070 temperature, and productivity on the hydrogen isotope signatures of lipid
1071 biomarkers. *Biogeosciences* **14**, 3979–3994.
1072 Ladd S. N., Nelson D. B., Schubert C. J. and Dubois N. (2018) Lipid compound classes
1073 display diverging hydrogen isotope responses in lakes along a nutrient gradient.
1074 *Geochim. Cosmochim. Acta* **237**, 103–119.
1075 Leavitt W. D., Flynn T. M., Suess M. K. and Bradley A. S. (2016) Transhydrogenase
1076 and growth substrate influence lipid hydrogen isotope ratios in *Desulfovibrio*
1077 *alaskensis* G20. *Front. Microbiol.* **7**, 918.
1078 Leavitt W. D., Murphy S. J. L., Lynd L. R. and Bradley A. S. (2017) Hydrogen isotope
1079 composition of *Thermoanaerobacterium saccharolyticum* lipids: Comparing wild
1080 type with a *nfn*-transhydrogenase mutant. *Org. Geochem.* **113**, 239–241.
1081 Lengger S. K., Rush D., Mayser J. P., Blewett J., Schwartz-Narbonne R., Talbot H. M.,
1082 Middelburg J. J., Jetten M. S. M., Schouten S., Sinninghe Damsté J. S. and Pancost
1083 R. D. (2019) Dark carbon fixation in the Arabian Sea oxygen minimum zone
1084 contributes to sedimentary organic carbon (SOM). *Global Biogeochem. Cy.* **33**,
1085 1715–1732.
1086 Li C., Sessions A. L., Kinnaman F. S. and Valentine D. L. (2009) Hydrogen-isotopic
1087 variability in lipids from Santa Barbara Basin sediments. *Geochim. Cosmochim.*
1088 *Acta* **73**, 4803–4823.

1089 Li J., Li J., Dang H., Jiang M. (2007) Vegetation and conservation strategy of Dajiuhu
1090 wetland park in Shennongjia region. *J. Wuhan Bot. Res.* **25**, 605–611 (in Chinese
1091 with English abstract).
1092 Lichtenthaler H. (1999) The 1-deoxy-D-xylulose-5-phosphate pathway of isoprenoid
1093 biosynthesis in plants. *Annu. Rev. Plant Physiol. Plant Mol. Biol.* **50**, 47–65.
1094 Londry K. L., Jahnke L. L. and des Marais D. J. (2004) Stable carbon isotope ratios of
1095 lipid biomarkers of sulfate-reducing bacteria. *Appl. Environ. Microbiol.* **70**, 745–
1096 751.
1097 Londry K. L., Dawson K. G., Grover H. D., Summons R. E. and Bradley A. S. (2008)
1098 Stable carbon isotope fractionation between substrates and products of
1099 *Methanosarcina barkeri*. *Org. Geochem.* **39**, 608–621.
1100 Luo T., Lun Z. J., Gu Y. S., Qin Y. M., Zhang Z. and Zhang B. (2015) Plant community
1101 survey and ecological protection of Dajiuhu Wetlands in Shengnongjia Area.
1102 *Wetland Sci.* **13**, 153–160 (in Chinese with English abstract).
1103 McFarlin J. M., Axford Y., Kusch S., Masterson A. L., Lasher G. E. and Osburn M. R.
1104 (2023) Aquatic plant wax hydrogen and carbon isotopes in Greenland lakes record
1105 shifts in methane cycling during past Holocene warming. *Sci. Adv.* **9**, eadh9704.
1106 Mills C. T., Amano Y., Slater G. F., Dias R. F., Iwatsuki T. and Mandernack K. W. (2010)
1107 Microbial carbon cycling in oligotrophic regional aquifers near the Tono Uranium
1108 Mine, Japan as inferred from $\delta^{13}C$ and $\Delta^{14}C$ values of in situ phospholipid fatty
1109 acids and carbon sources. *Geochim. Cosmochim. Acta* **74**, 3785–3805.
1110 Monson K. D. and Hayes J. M. (1982) Carbon isotopic fractionation in the biosynthesis

of bacterial fatty acids. Ozonolysis of unsaturated fatty acids as a means of determining the intramolecular distribution of carbon isotopes. *Geochim. Cosmochim. Acta* **46**, 139–149.

Musat F., Vogt C. and Richnow H. H. (2016) Carbon and hydrogen stable isotope fractionation associated with the aerobic and anaerobic degradation of saturated and alkylated aromatic hydrocarbons. *J. Mol. Microbiol. Biotechnol.* **26**, 211–226.

Naafs B. D. A., Inglis G. N., Blewett J., McClymont E. L., Lauretano V., Xie S., Evershed R. P. and Pancost R. D. (2019) The potential of biomarker proxies to trace climate, vegetation, and biogeochemical processes in peat: A review. *Glob. Planet. Change* **179**, 57–79.

Naraoka H., Uehara T., Hanada S. and Kakegawa T. (2010) δ^{13}C-δD distribution of lipid biomarkers in a bacterial mat from a hot spring in Miyagi Prefecture, NE Japan. *Org. Geochem.* **41**, 398–403.

Nichols P. D., Guckert J. B. and White D. C. (1986) Determination of monosaturated fatty acid double-bond position and geometry for microbial monocultures and complex consortia by capillary GC-MS of their dimethyl disulphide adducts. *J. Microbiol. Methods* **5**, 49–55.

Ohlrogge J. and Browse J. (1995) Lipid biosynthesis. *Plant Cell* **7**, 957.

Osburn M. R., Sessions A. L., Pepe-Ranney C. and Spear J. R. (2011) Hydrogen-isotopic variability in fatty acids from Yellowstone National Park hot spring microbial communities. *Geochim. Cosmochim. Acta* **75**, 4830–4845.

Osburn M. R., Dawson K. S., Fogel M. L. and Sessions A. L. (2016) Fractionation of

1133 hydrogen isotopes by sulfate-and nitrate-reducing bacteria. *Front. Microbiol.* **7**,
1134 1166.
1135 Pan X., He Y., Yan M., Ji Z., Li T., Yan R., Zhou C. and Wang J. M. (2013) Analysis on
1136 current situation of hydrology and water resources and protection measures of Dajiu
1137 Lake in Shenlongjia. *Hubei Agric. Sci* **52**, 3033–3037 (in Chinese with English
1138 abstract)
1139 Pancost R. D. and Sinninghe Damsté J. S. (2003) Carbon isotopic compositions of
1140 prokaryotic lipids as tracers of carbon cycling in diverse settings. *Chem. Geol.* **195**,
1141 29–58.
1142 Pancost R. D., Pressley S., Coleman J. M., Talbot H. M., Kelly S. P., Farrimond P.,
1143 Schouten S., Benning L. and Mountain B. W. (2006) Composition and implications
1144 of diverse lipids in New Zealand geothermal sinters. *Geobiology* **4**, 71–92.
1145 Pancost R. D., Steart D. S., Handley L., Collinson M. E., Hooker J. J., Scott, A. C.,
1146 Grassineau N. V. and Glasspool I. J. (2007) Increased terrestrial methane cycling at
1147 the Palaeocene–Eocene thermal maximum. *Nature* **449**, 332–335.
1148 Pelz O., Abraham W. R., Saurer M., Siegwolf R. and Zeyer J. (2005) Microbial
1149 assimilation of plant-derived carbon in soil traced by isotope analysis. *Biol. Fertil.*
1150 *Soils* **41**, 153–162.
1151 Petsch S. T., Edwards K. J. and Eglinton T. I. (2003) Abundance, distribution and $\delta^{13}C$
1152 analysis of microbial phospholipid-derived fatty acids in a black shale weathering
1153 profile. *Org. Geochem.* **34**, 731–743.
1154 Praeg N., Wagner A. O. and Illmer P. (2014) Effects of fertilisation, temperature and

1155 water content on microbial properties and methane production and methane
1156 oxidation in subalpine soils. *Eur. J. Soil Biol.* **65**, 96–106.
1157 Reddy K. R., DeLaune R. D. and Inglett P. W. (2022) Biogeochemistry of Wetlands:
1158 Science and Applications (Second Edition). CRC Press, Boca Raton.
1159 Sachse D., Billault I., Bowen G. J., Chikaraishi Y., Dawson T. E., Feakins S. J., Freeman
1160 K. H., Magill C. R., McInerney F. A., van der Meer M. T. J., Polissar P., Robins R.
1161 J., Sachs J. P., Schmidt H.-L., Sessions A. L., White J. W. C., West J. B. and Kahmen
1162 A. (2012) Molecular paleohydrology: interpreting the hydrogen-isotopic
1163 composition of lipid biomarkers from photosynthesizing organisms. *Annu. Rev.*
1164 *Earth Planet. Sci.* **40**, 221–249.
1165 Saito K, Kawaguchi A, Okuda S, Seyama Y, Yamakawa T (1980) Incorporation of
1166 hydrogen atoms from deuterated water and stereospecifically deuterium-labeled
1167 nicotinamide nucleotides into fatty acids with the Escherichia coli fatty acid
1168 synthetase system. *Biochim. Biophys. Acta* **618**, 202–213.
1169 Sakata S., Hayes J. M., McTaggart A. R., Evans R. A., Leckrone K. J. and Togasaki R.
1170 K. (1997) Carbon isotopic fractionation associated with lipid biosynthesis by a
1171 cyanobacterium: relevance for interpretation of biomarker records. *Geochim.*
1172 *Cosmochim. Acta* **61**, 5379–5389.
1173 Seifert A. G., Trumbore S., Xu X., Zhang D. and Gleixner G. (2013) Variable effects of
1174 plant colonization on black slate uptake into microbial PLFAs. *Geochim.*
1175 *Cosmochim. Acta* **106**, 391–403.
1176 Sessions A. L., Burgoyne T. W., Schimmelmann A. and Hayes J. M. (1999)

1177 Fractionation of hydrogen isotopes in lipid biosynthesis. *Org. Geochem.* **30**, 1193–
1178 1200.
1179 Sessions A. L., Jahnke L. L., Schimmelmann A. and Hayes J. M. (2002) Hydrogen
1180 isotope fractionation in lipids of the methane-oxidizing bacterium *Methylococcus*
1181 *capsulatus*. *Geochim. Cosmochim. Acta* **66**, 3955–3969.
1182 Sessions A. L., Sylva S. P., Summons R. E. and Hayes J. M. (2004). Isotopic exchange
1183 of carbon-bound hydrogen over geologic timescales. *Geochim. Cosmochim. Acta*
1184 **68**, 1545–1559.
1185 Sessions A. L. (2006) Seasonal changes in D/H fractionation accompanying lipid
1186 biosynthesis in *Spartina alterniflora*. *Geochim. Cosmochim. Acta* **70**, 2153–2162.
1187 Sessions A. L. (2016) Factors controlling the deuterium contents of sedimentary
1188 hydrocarbons. *Org. Geochem.* **96**, 43–64.
1189 Schirmer A., Rude M. A., Li X., Popova E. and Del Cardayre S. B. (2010) Microbial
1190 biosynthesis of alkanes. *Science* **329**, 559–562.
1191 Schmidt H. L., Werner R. A. and Eisenreich W. (2003) Systematics of ^{2}H patterns in
1192 natural compounds and its importance for the elucidation of biosynthetic pathways.
1193 *Phytochem. Rev.* **2**, 61–85.
1194 Schouten S., Strous M., Kuypers M. M., Rijpstra W. I. C., Baas M., Schubert C. J.,
1195 Jetten M. S. M. and Sinninghe Damsté J. S. (2004) Stable carbon isotopic
1196 fractionations associated with inorganic carbon fixation by anaerobic ammonium-
1197 oxidizing bacteria. *Appl. Environ. Microbiol.* **70**, 3785–3788.
1198 Simkus D. N., Slater G. F., Lollar B. S., Wilkie K., Kieft T. L., Magnabosco C., Lau M.

1199 C. Y., Pullin M. J., Hendrickson S. B., Wommack K. E., Sakowski E. G., van
1200 Heerden E., Kuloyo O., Linage B., Borgonie G. and Onstott, T. C. (2016) Variations
1201 in microbial carbon sources and cycling in the deep continental subsurface.
1202 *Geochim. Cosmochim. Acta* **173**, 264–283.
1203 Smith F. A. and Freeman K. H. (2006) Influence of physiology and climate on δD of
1204 leaf wax *n*-alkanes from C_3 and C_4 grasses. *Geochim. Cosmochim. Acta* **70**, 1172–
1205 1187.
1206 Stemmer M., Watzinger A., Blochberger K., Haberhauer G. and Gerzabek M. H. (2007)
1207 Linking dynamics of soil microbial phospholipid fatty acids to carbon
1208 mineralization in a ^{13}C natural abundance experiment: Impact of heavy metals and
1209 acid rain. *Soil Biol. Biochem.* **39**, 3177–3186.
1210 Summons R. E., Jahnke L. L. and Roksandic Z. (1994) Carbon isotopic fractionation in
1211 lipids from methanotrophic bacteria: relevance for interpretation of the geochemical
1212 record of biomarkers. *Geochim. Cosmochim. Acta* **58**, 2853–2863.
1213 Talbot H. M., Bischoff J., Inglis G. N., Collinson M. E. and Pancost R. D. (2016)
1214 Polyfunctionalised bio-and geohopanoids in the Eocene Cobham Lignite. *Org.*
1215 *Geochem.* **96**, 77–92.
1216 Valentine D. L., Sessions A. L., Tyler S. C. and Chidthaisong A. (2004) Hydrogen
1217 isotope fractionation during H_2/CO_2 acetogenesis: hydrogen utilization efficiency
1218 and the origin of lipid-bound hydrogen. *Geobiology* **2**, 179–188.
1219 Valentine D. L. (2009) Isotopic remembrance of metabolism past. *Proc. Natl. Acad. Sci.*
1220 *U.S.A.* **106**, 12565–12566.

1221 Vestal J. R. and White D. C. (1989) Lipid analysis in microbial ecology. *Bioscience* **39**,
1222 535–541.
1223 Vogt C., Cyrus E., Herklotz I., Schlosser D., Bahr A., Herrmann S., Richnow H. H. and
1224 Fischer A. (2008) Evaluation of toluene degradation pathways by two-dimensional
1225 stable isotope fractionation. *Environ. Sci. Technol.* **42**, 7793–7800.
1226 van Dongen B. E., Schouten S. and Sinninghe Damsté J. S. (2001) Gas
1227 chromatography/combustion/isotope-ratio-monitoring mass spectrometric analysis
1228 of methylboronic derivatives of monosaccharides: a new method for determining
1229 natural ^{13}C abundances of carbohydrates. *Rapid Commun. Mass Spectrom.* **15**, 496–
1230 500.
1231 van Dongen B. E., Schouten S. and Sinninghe Damsté J. S. (2002) Carbon isotope
1232 variability in monosaccharides and lipids of aquatic algae and terrestrial plants. *Mar.*
1233 *Ecol. Prog. Ser.* **232**, 83–92.
1234 van der Meer M. T. J., Schouten S. and Sinninghe Damsté J. S. (1998) The effect of the
1235 reversed tricarboxylic acid cycle on the ^{13}C contents of bacterial lipids. *Org.*
1236 *Geochem.* **28**, 527–533.
1237 van der Meer M. T. J., Schouten S., van Dongen B. E., Rijpstra W. I. C., Fuchs G.,
1238 Sinninghe Damsté J. S., de Leeuw J. W. and Ward D. M. (2001) Biosynthetic
1239 controls on the ^{13}C contents of organic components in the photoautotrophic
1240 bacterium *Chloroflexus aurantiacus*. *J. Biol. Chem.* **276**, 10971–10976.
1241 van Winden J. F., Kip N., Reichart G., Jetten M. S. M., Op den Camp H. J. M. and
1242 Sinninghe Damsté J. S. (2010) Lipids of symbiotic methane-oxidizing bacteria in

peat moss studied using stable carbon isotopic labelling. *Org. Geochem.* **41**, 1040–1044.

van Winden J. F., Talbot H. M., Kip N., Reichart G. J., Pol A., McNamara N. P., Jetten M. S. M., Op den Camp H. J. M. and Sinninghe Damsté, J. S. (2012) Bacteriohopanepolyol signatures as markers for methanotrophic bacteria in peat moss. *Geochim. Cosmochim. Acta* **77**, 52–61.

Watzinger A., Stemmer M., Pfeffer M., Rasche F. and Reichenauer T. G. (2008) Methanotrophic communities in a landfill cover soil as revealed by [^{13}C] PLFAs and respiratory quinones: Impact of high methane addition and landfill leachate irrigation. *Soil Biol. Biochem.* **40**, 751–762.

Watzinger A., Feichtmair S., Kitzler B., Zehetner F., Kloss S., Wimmer B., Zechmeister-Boltenstern S. and Soja G. (2014) Soil microbial communities responded to biochar application in temperate soils and slowly metabolized ^{13}C-labelled biochar as revealed by ^{13}C PLFA analyses: results from a short-term incubation and pot experiment. *Eur. J. Soil Sci.* **65**, 40–51.

Watzinger A. (2015) Microbial phospholipid biomarkers and stable isotope methods help reveal soil functions. *Soil Biol. Biochem.* **86**, 98–107.

Wei T. and Simko V. (2021) R package 'corrplot': Visualization of a Correlation Matrix (Version 0.92).

White D. C., Davis W. M., Nickels J. S., King J. D. and Bobbie R. J. (1979) Determination of the sedimentary microbial biomass by extractible lipid phosphate. *Oecologia* **40**, 51–62.

1265 Wijker R. S., Sessions A. L., Fuhrer T. and Phan M. (2019) $^{2}H/^{1}H$ variation in microbial
1266 lipids is controlled by NADPH metabolism. *Proc. Natl. Acad. Sci. U.S.A.* **116**,
1267 12173–12182.
1268 Xiang X., Wang H., Tian W., Wang R., Gong L., Xu Y. and Man B. (2023) Composition
1269 and function of bacterial communities of bryophytes and their underlying sediments
1270 in the Dajiuhu Peatland, central China. *J. Earth Sci.* **34**, 133–144.
1271 Yan C., Zhang Y., Zhang Y., Zhang Z. and Huang X. (2020) Habitat influence on the
1272 molecular, carbon and hydrogen isotope compositions of leaf wax *n*-alkanes in a
1273 subalpine basin, central China. *J. Earth Sci.* **31**, 845–852.
1274 Zelles L. (1997) Phospholipid fatty acid profiles in selected members of soil microbial
1275 communities. *Chemosphere* **35**, 275–294.
1276 Zelles L. (1999) Fatty acid patterns of phospholipids and lipopolysaccharides in the
1277 characterisation of microbial communities in soil: A review. *Biol. Fertil. Soils* **29**,
1278 111–129.
1279 Zhang C. L., Li Y., Wall J. D., Larsen L., Sassen R., Huang Y., Wang Y., Peacock A.,
1280 White D. C., Horita J. and Cole D. R. (2002) Lipid and carbon isotopic evidence of
1281 methane-oxidizing and sulfate-reducing bacteria in association with gas hydrates
1282 from the Gulf of Mexico. *Geology* **30**, 239–242.
1283 Zhang C. L., Li Y., Ye Q., Fong J., Peacock A. D., Blunt E., Fang J., Lovley D. R. and
1284 White D. C. (2003) Carbon isotope signatures of fatty acids in *Geobacter*
1285 *metallireducens* and *Shewanella algae*. *Chem. Geol.* **195**, 17–28.
1286 Zhang C. L., Fouke B. W., Bonheyo G. T., Peacock A. D., White D. C., Huang Y. and

1287 Romanek C. S. (2004) Lipid biomarkers and carbon-isotopes of modern travertine
1288 deposits (Yellowstone National Park, USA): implications for biogeochemical
1289 dynamics in hot-spring systems. *Geochim. Cosmochim. Acta* **68**, 3157–3169.
1290 Zhang C. L., Huang Z., Cantu J., Pancost R. D., Brigmon R. L., Lyons T. W. and Sassen
1291 R. (2005) Lipid biomarkers and carbon isotope signatures of a microbial (Beggiatoa)
1292 mat associated with gas hydrates in the Gulf of Mexico. *Appl. Environ. Microbiol.*
1293 **71**, 2106–2112.
1294 Zhang X., Gillespie A. L. and Sessions A. L. (2009) Large D/H variations in bacterial
1295 lipids reflect central metabolic pathways. *Proc. Natl. Acad. Sci. U.S.A.* **106**, 12580–
1296 12586.
1297 Zhang Z. and Sachs J. P. (2007) Hydrogen isotope fractionation in freshwater algae: I.
1298 Variations among lipids and species. *Org. Geochem.* **38**, 582–608.
1299 Zhang Y., Zheng N., Wang J., Yao H., Qiu Q. and Chapman S. J. (2019) High turnover
1300 rate of free phospholipids in soil confirms the classic hypothesis of PLFA
1301 methodology. *Soil Biol. Biochem.* **135**, 323–330.
1302 Zhang Y., Huang X., Wang R. and Naafs B. D. A. (2020) The distribution of long-chain
1303 *n*-alkan-2-ones in peat can be used to infer past changes in pH. *Chem. Geol.* **544**,
1304 119622.
1305 Zhang Y., Huang X., Zhang Z., Blewett J. and Naafs, B. D. A. (2022a) Spatiotemporal
1306 dynamics of dissolved organic carbon in a subtropical wetland and their
1307 implications for methane emissions. *Geoderma* **419**, 115876.
1308 Zhang Y., Naafs B.D.A., Huang X., Song Q., Xue J., Wang R., Zhao M., Evershed R.P.,

1309 Pancost R.D. and Xie S. (2022b) Variations in wetland hydrology drive rapid
1310 changes in the microbial community, carbon metabolic activity, and greenhouse gas
1311 fluxes. *Geochim. Cosmochim. Acta* **317**, 269–285.
1312 Zhao B., Zhang Y., Huang X., Qiu R., Zhang Z. and Meyers P. A. (2018) Comparison
1313 of *n*-alkane molecular, carbon and hydrogen isotope compositions of different types
1314 of plants in the Dajiuhu peatland, Central China. *Org. Geochem.* **124**, 1–11.
1315 Zhao W., Fang J., Huang X., Zhang Y., Liu W., Wang Y. and Zhang L. (2020a) Carbon
1316 and hydrogen isotope fractionation in lipid biosynthesis by *Sporosarcina* sp. DSK25.
1317 *Geochem. Persp. Let.* **14**, 9–13.
1318 Zhao M., Zhang Y., Zhang Z., Huang X. (2020b) Comparison of microbial community
1319 in topsoil among different habitats in Dajiuhu, Hubei Province: Evidence from
1320 phospholipid fatty acids. *Earth Sci.* **45**, 1877–1886 (in Chinese with English
1321 abstract).
1322 Ziolkowski L. A., Wierzchos J., Davila A. F. and Slater G. F. (2013) Radiocarbon
1323 evidence of active endolithic microbial communities in the hyperarid core of the
1324 Atacama Desert. *Astrobiology* **13**, 607–616.
1325

Figure Captions

Fig. 1. (a) Map for the location of the Dajiuhu Basin. (b) Geomorphological maps and distribution of sampling sites in the Dajiuhu Basin. The photographs on the right show the three main habitats within the basin. The base map in (a) was downloaded from https://ngdc.noaa.gov/mgg/global/relief/ETOPO1/image.

Fig. 2. Cluster analysis of the PLFA fractional abundance and microbial community structure across the three habitats. The numbers on the left represent sample locations (as shown in Fig. 1). Data were obtained from the previous study (Zhao et al., 2020b).

Fig. 3. (a) The $\delta^{13}C$ values of microbial PLFAs in the three habitats. The horizontal dashed line and gray shade represent the average $\delta^{13}C_{bulk}$ value with 1σ of 0.7 across all samples. (b) The offset between $\delta^{13}C$ of PLFAs and bulk organic carbon ($\varepsilon C_{FA/bulk}$). The horizontal dashed line represents $\varepsilon C_{FA/bulk}$ = 0 ‰. All error bars reflect one standard deviation (±1σ) between multiple samples in different habitats.

Fig. 4. (a) The $\delta^{2}H$ values of microbial PLFAs across the three habitats. (b) The offset between $\delta^{2}H$ of PLFAs and soil water ($\varepsilon H_{FA/water}$). The horizontal dashed line ($\varepsilon H_{FA/water}$ = -160 ‰) represents the theoretical boundary between heterotrophy and autotrophy based on culture experiments. All error bars reflect one standard deviation (±1σ) between multiple samples in different habitats.

Fig. 5. Correlation heat map showing the correlation efficiencies between the (a) $\delta^{13}C$ and $\delta^{2}C$, (b) $\varepsilon C_{FA/bulk}$ and $\varepsilon H_{FA/water}$, and environmental parameters. SWC = soil water content. ST = soil temperature. One and two white asterisks represent significant correlations at the 0.05 and 0.01 levels, respectively, while the cross represents no significant correlation ($p > 0.05$).

Fig. 6. Correlations between carbon and hydrogen isotope composition of fatty acids. (a) $\delta^{13}C$ versus $\delta^{2}H$ of PLFAs 16:0 and 18:0. (b) $\delta^{13}C$ versus $\delta^{2}H$ of PLFAs i15:0, a15:0, and i16:0. (c) $\delta^{13}C$ versus $\delta^{2}H$ of PLFAs 16:1ω7c, 18:1ω7c, and 18:1ω9c. (d) $\delta^{13}C$ versus $\delta^{2}H$ of all PLFAs in the three habitats. (e) $\varepsilon C_{FA/bulk}$ versus $\varepsilon H_{FA/water}$ of all PLFAs in the three habitats. (f) α_C^{-1}-1 versus α_H^{-1}-1 of all PLFAs in the three habitats, from which the linear regression slope can be derived (in the equations) . The error of the slope is shown in parentheses. (g) $\delta^{13}C$ versus $\delta^{2}H$ of 16:0 fatty acid from peats/soils (this study) and marine surface sediments (Allan et al., 2023). (h) $\varepsilon C_{FA/bulk}$ versus $\varepsilon H_{FA/water}$ of 16:0 fatty acid from peats/soils (this study) and marine surface sediments (Allan et al., 2023). (i) Comparison of $\varepsilon H_{FA/water}$ of short-chain fatty acids (C_{14}-C_{19}) in peats/soils (this study) and lake and marine environments. Lake and marine data cited from Sessions et al. (1999), Jones et al. (2008), Li et al. (2009), Heinzelmann et al. (2016), Ladd et al. (2017), Heinzelmann et al. (2018), Ladd et al. (2018), Chen et al. (2021), Häggi et al. (2021), and Allan et al. (2023). Note that some marine samples only have $\delta^{2}H$ values and were calculated to $\varepsilon H_{FA/water}$ by assuming a seawater $\delta^{2}H$ value of ~ 0 ‰.

Fig. 7. (a) δ^2H of soil water in the Dajiuhu basin collected in June 2018 (n = 22, this study). (b) δ^2H of soil water in the peatland of the Dajiuhu basin during the growing season (April to October) from 2015 to 2017 (n = 164). Data cited from Huang et al. (2018), Zhao et al. (2018), and Huang and Meyers. (c) δ^2H of soil water in the growing season simulated based on soil evaporation model (Smith and Freeman, 2006) and meteoric water δ^2H values. (d) δ^2H of meteoric water during the growing season. The data were obtained from measured values from April to October at Wuhan and Chongqing stations in the Global Network of Isotopes in Precipitation (GNIP) (IAEA/WMO, 2023), as well as calculated monthly values using the Online Isotopes in Precipitation Calculator (OIPC) (Bowen et al., 2005; Bowen, 2023) by inputting coordinates and elevation of the Dajiuhu basin. The white square represents the average value in each box-whisker plot.

1383 **Table 1**. Environmental and bulk geochemical results of topsoil samples from three habitats. We used the average value of these parameters from

1384 all samples, with ± indicating one standard deviation (±1σ). ST = soil temperature; SWC = soil water content. Significant differences in results

1385 across habitats are indicated by * ($p < 0.05$) and ** ($p < 0.01$).

1386

Habit	ST (°C)	SWC** (%)	pH*	NH_4^+-N (mg/L)	NO_3^--N* (mg/L)	TOC** (%)	C/N*	$\delta^{13}C_{bulk}$ (‰)	$\delta^{2}H_{water}$** (‰)
peatland	17.2±3.0	86±9	4.0±0.2	2.9±1.1	0.11±0.08	19.5±3.7	17.2±2.5	-28.4±0.7	-39.9±5.4
meadow	19.3±1.4	42±12	4.6±0.1	2.9±0.8	0.65±0.60	6.1±2.1	17.2±5.9	-28.0±0.7	-49.2±9.2
woodland	18.0±0.0	48±3	4.8±1.3	3.5±1.8	0.08±0.08	9.1±0.9	25.2±8.5	-27.8±0.7	-52.9±2.7

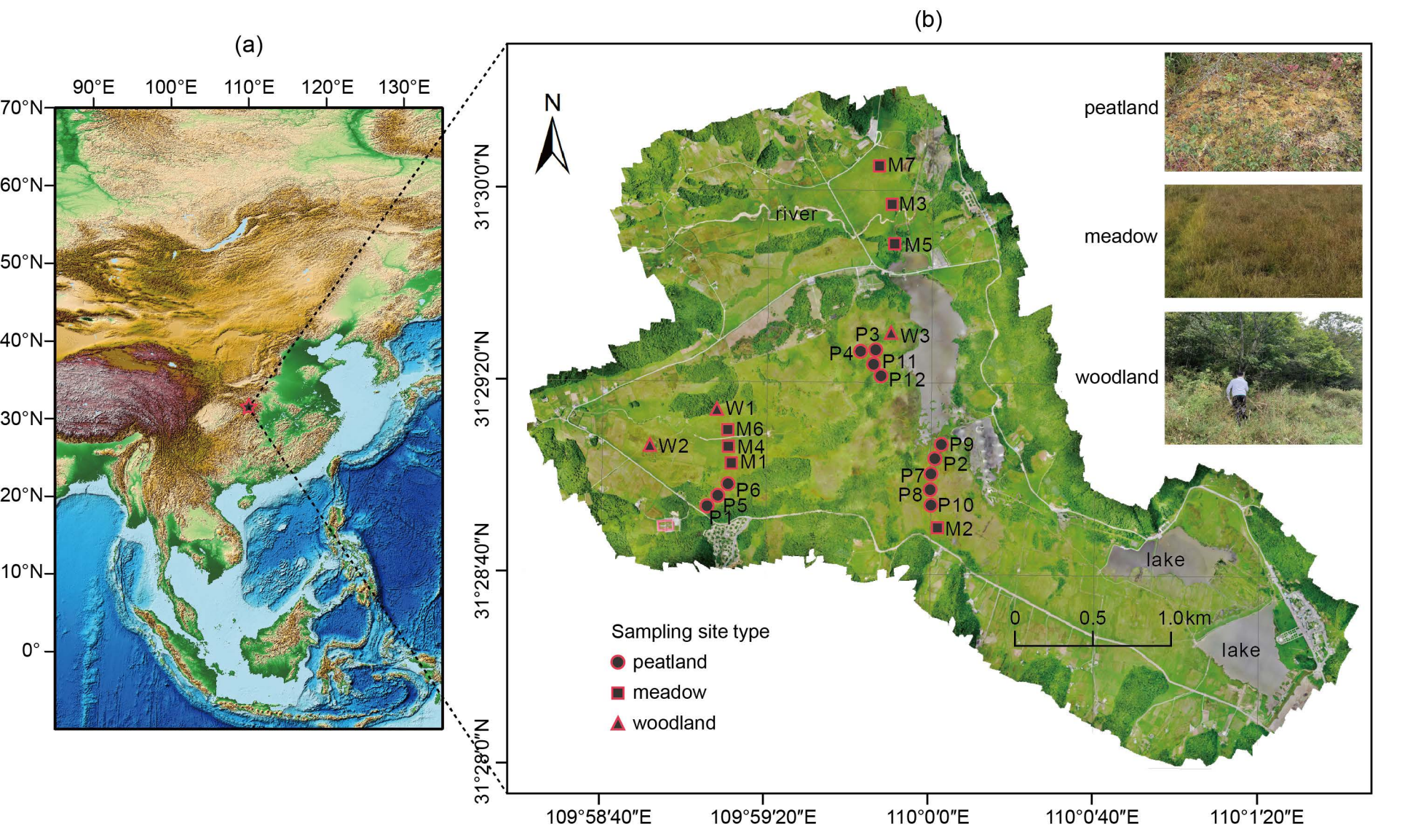
(a)
90°E
100°E
110°E
120°E
130°E
70°N
60°N
50°N
40°N
30°N
20°N
10°N
0°
(b)
N
peatland
meadow
woodland
river
M7
M3
M5
P3
W3
P4
P11
P12
W1
M6
W2
M4
M1
P6
P5
P1
P9
P2
P7
P8
P10
M2
lake
lake
0
0.5
1.0km
Sampling site type
peatland
meadow
woodland
31°30′0″N
31°29′20″N
31°28′40″N
31°28′0″N
109°58′40″E
109°59′20″E
110°0′0″E
110°0′40″E
110°1′20″E

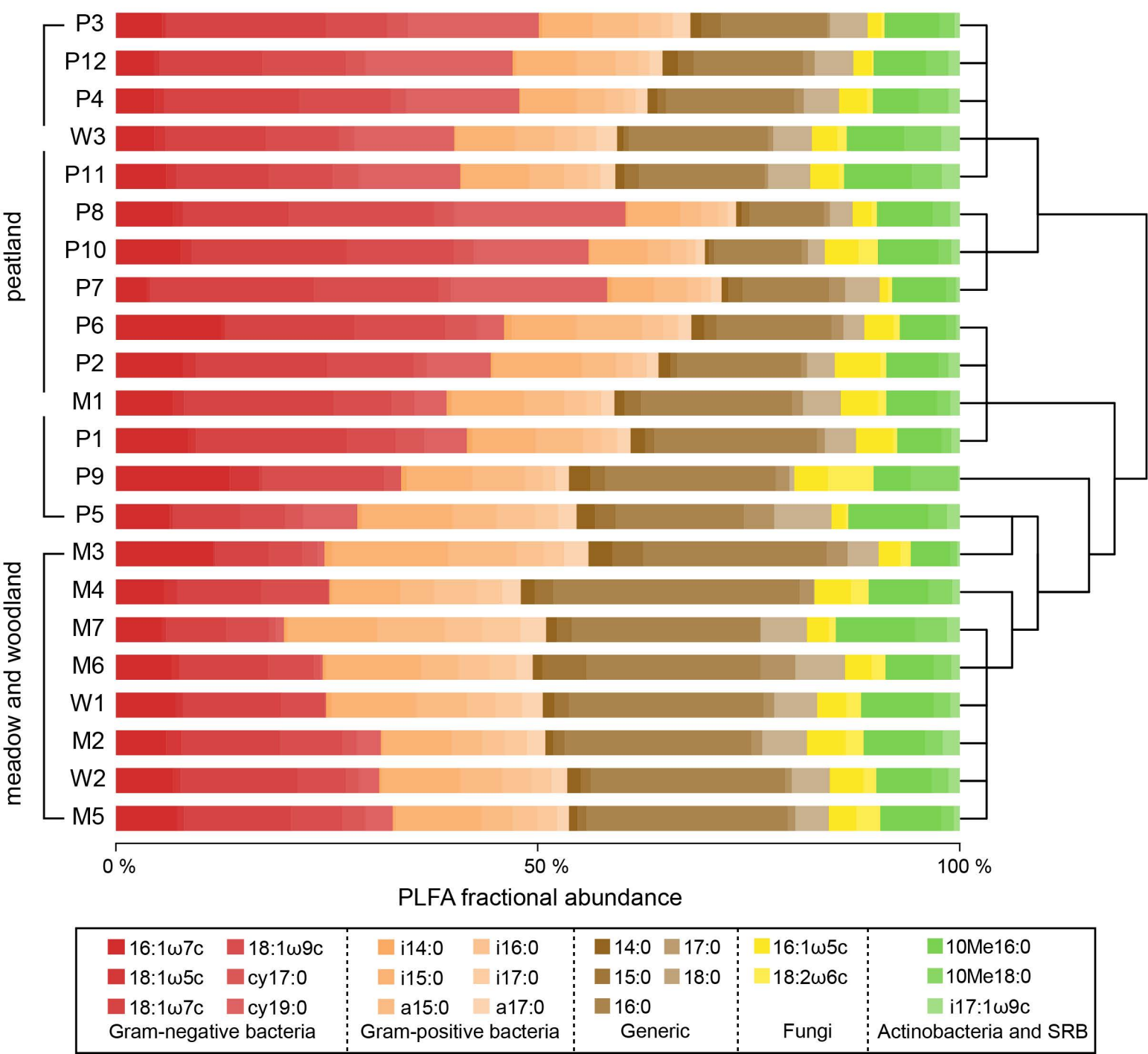
P3
P12
P4
W3
P11
P8
P10
P7
P6
P2
M1
P1
P9
P5
M3
M4
M7
M6
W1
M2
W2
M5
peatland
meadow and woodland
0 %
50 %
100 %
PLFA fractional abundance
16:1ω7c
18:1ω9c
18:1ω5c
cy17:0
18:1ω7c
cy19:0
Gram-negative bacteria
i14:0
i16:0
i15:0
i17:0
a15:0
a17:0
Gram-positive bacteria
14:0
17:0
15:0
18:0
16:0
Generic
16:1ω5c
18:2ω6c
Fungi
10Me16:0
10Me18:0
i17:1ω9c
Actinobacteria and SRB

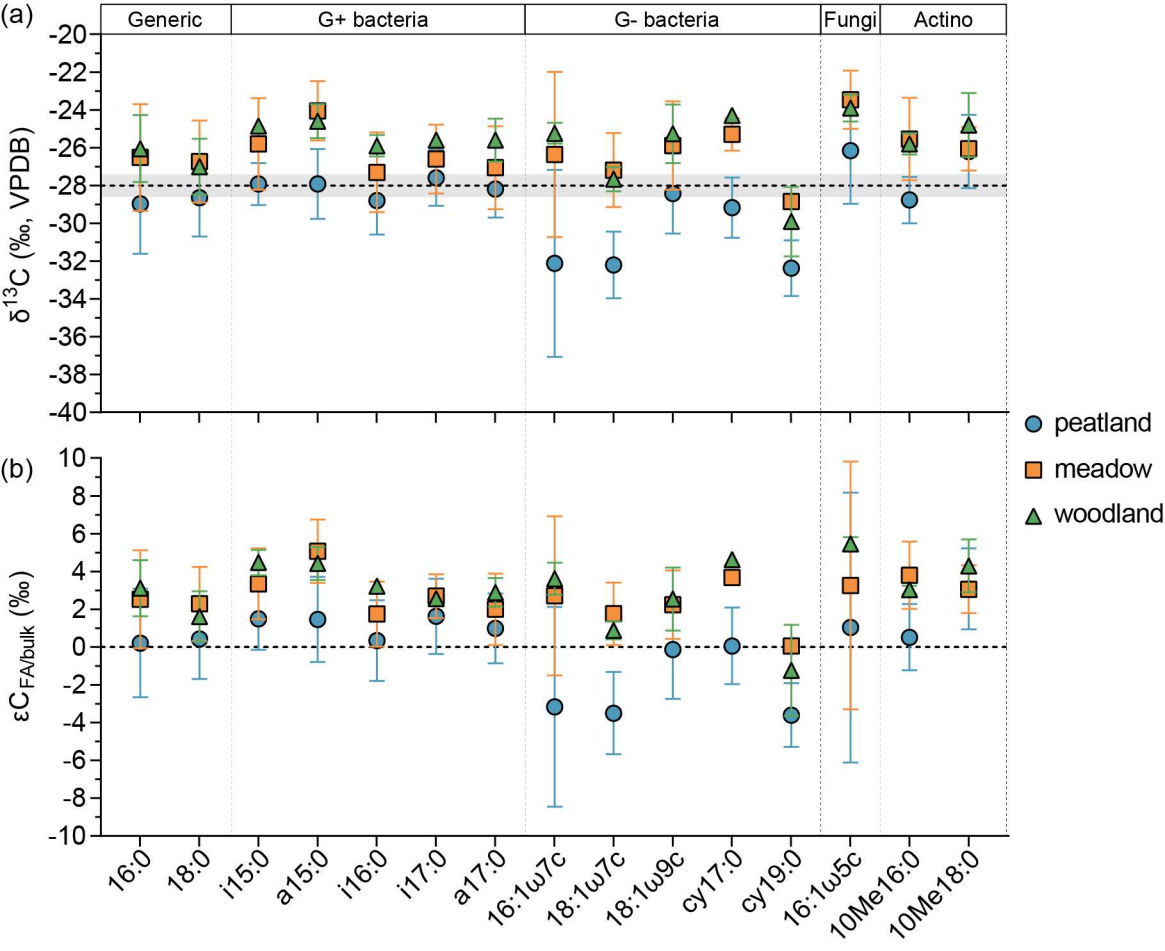
(a)
Generic
G+ bacteria
G- bacteria
Fungi
Actino
δ13C (‰, VPDB)
-20
-22
-24
-26
-28
-30
-32
-34
-36
-38
-40
peatland
meadow
woodland
(b)
εCFA/bulk (‰)
10
8
6
4
2
0
-2
-4
-6
-8
-10
16:0
18:0
i15:0
a15:0
i16:0
i17:0
a17:0
16:1ω7c
18:1ω7c
18:1ω9c
cy17:0
cy19:0
16:1ω5c
10Me16:0
10Me18:0

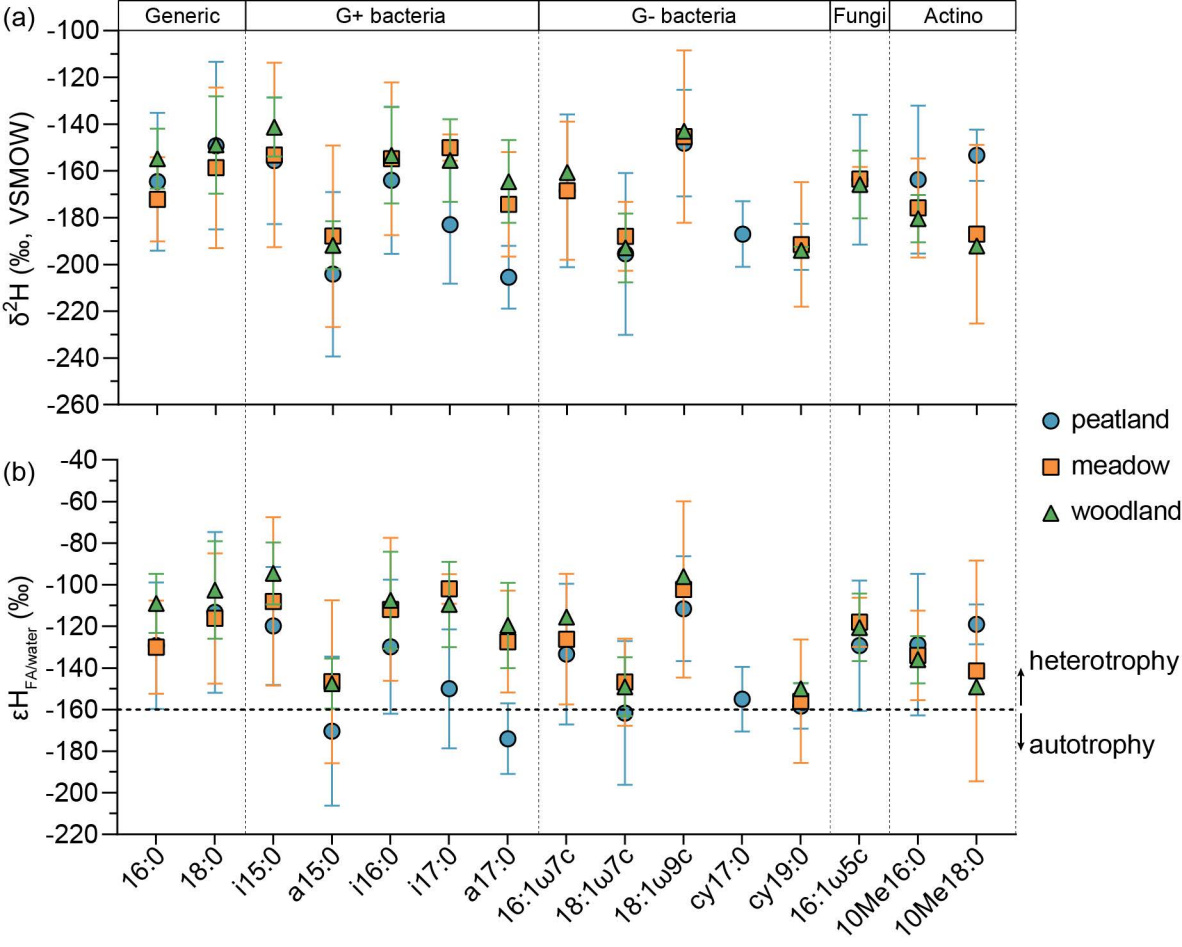
(a)
Generic
G+ bacteria
G- bacteria
Fungi
Actino
δ2H (‰, VSMOW)
-100
-120
-140
-160
-180
-200
-220
-240
-260
(b)
εHFA/water (‰)
-40
-60
-80
-100
-120
-140
-160
-180
-200
-220
peatland
meadow
woodland
heterotrophy
autotrophy
16:0
18:0
i15:0
a15:0
i16:0
i17:0
a17:0
16:1ω7c
18:1ω7c
18:1ω9c
cy17:0
cy19:0
16:1ω5c
10Me16:0
10Me18:0

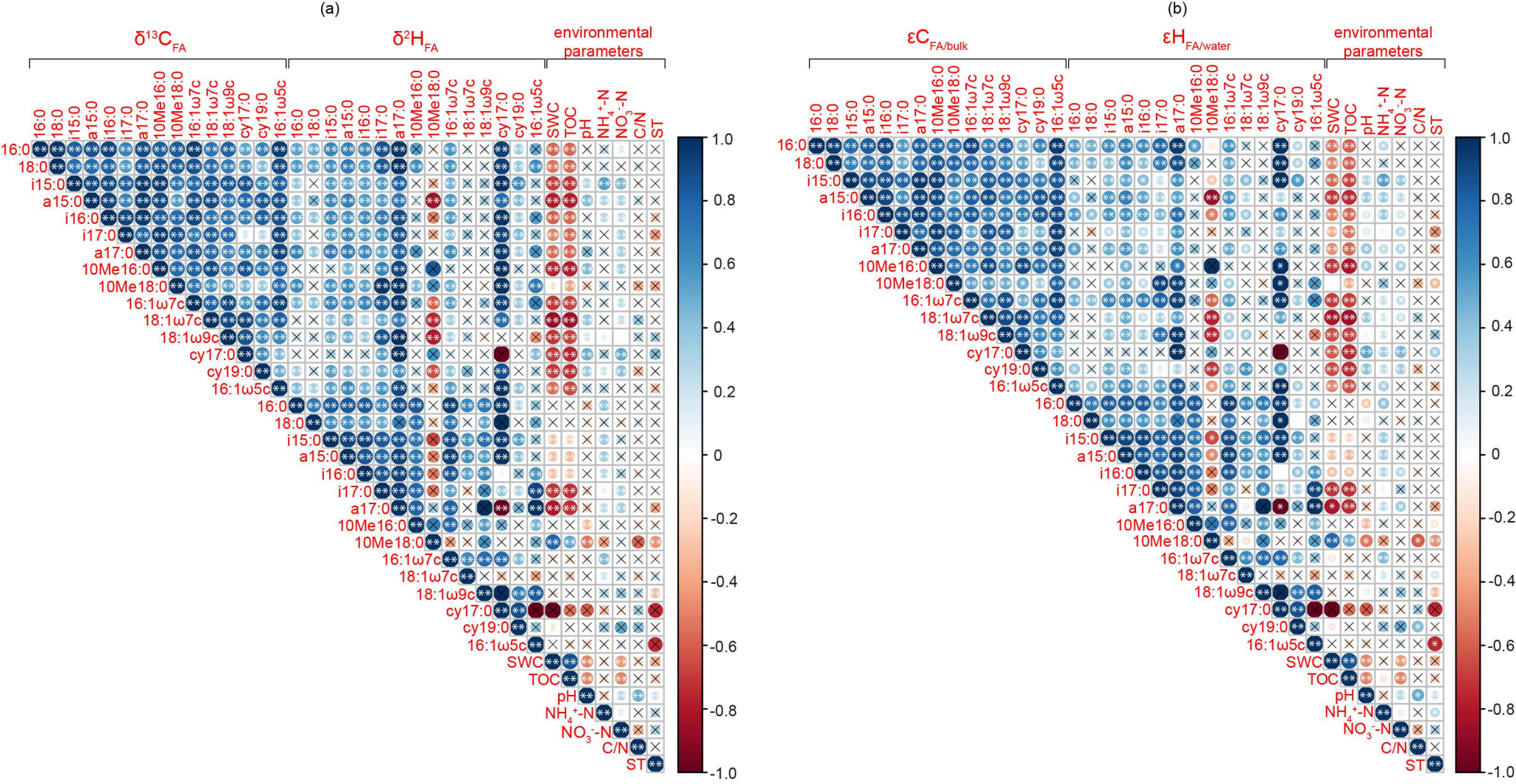
(a)
δ13CFA
δ2HFA
environmental parameters
16:0
18:0
i15:0
a15:0
i16:0
i17:0
a17:0
10Me16:0
10Me18:0
16:1ω7c
18:1ω7c
18:1ω9c
cy17:0
cy19:0
16:1ω5c
SWC
TOC
pH
NH4+-N
NO3--N
C/N
ST
1.0
0.8
0.6
0.4
0.2
0
-0.2
-0.4
-0.6
-0.8
-1.0
(b)
εCFA/bulk
εHFA/water
environmental parameters

(a)
r^2 = 0.3, p < 0.05 16:0
r^2 = 0.3, p < 0.05 18:0
δ^2H (‰, VSMOW)
δ^{13}C (‰, VPDB)

(b)
r^2 = 0.3, p < 0.05 i15:0
r^2 = 0.5, p < 0.01 a15:0
r^2 = 0.4, p < 0.05 i16:0
δ^2H (‰, VSMOW)
δ^{13}C (‰, VPDB)

(c)
r^2 = 0.3, p < 0.05 16:1ω7c
r^2 = 0.03, p > 0.05 18:1ω7c
r^2 = 0.02, p > 0.05 18:1ω9c
δ^2H (‰, VSMOW)
δ^{13}C (‰, VPDB)

(d)
r^2 = 0.2, p < 0.01 peatland
r^2 = 0.3, p < 0.01 meadow
r^2 = 0.2, p < 0.05 woodland
δ^2H (‰, VSMOW)
δ^{13}C (‰, VPDB)

(e)
r^2 = 0.2, p < 0.01 peatland
r^2 = 0.2, p < 0.01 meadow
r^2 = 0.2, p > 0.05 woodland
$\varepsilon H_{FA/water}$ (‰)
$\varepsilon C_{FA/bulk}$ (‰)

(f)
$y = 5.9x + 0.2$, r^2 = 0.2, p < 0.01, (±1.3)
$y = 6.4x + 0.2$, r^2 = 0.2, p < 0.01, (±2.2)
$y = 6.2x + 0.2$, r^2 = 0.2, p > 0.05, (±3.2)
peatland
meadow
woodland
α_H^{-1}-1
α_C^{-1}-1

(g)
r^2 = 0.3, p < 0.05 peats and soils
r^2 = 0.2, p < 0.05 marine surface sediments
δ^2H (‰, VSMOW)
δ^{13}C (‰, VPDB)

(h)
r^2 = 0.3, p < 0.05 peats and soils
r^2 = 0.2, p < 0.01 marine surface sediments
$\varepsilon H_{FA/water}$ (‰)
$\varepsilon C_{FA/bulk}$ (‰)

(i)
heterotrophy
autotrophy
$\varepsilon H_{FA/water}$ (‰)
peats and soils
lake environments
marine environments

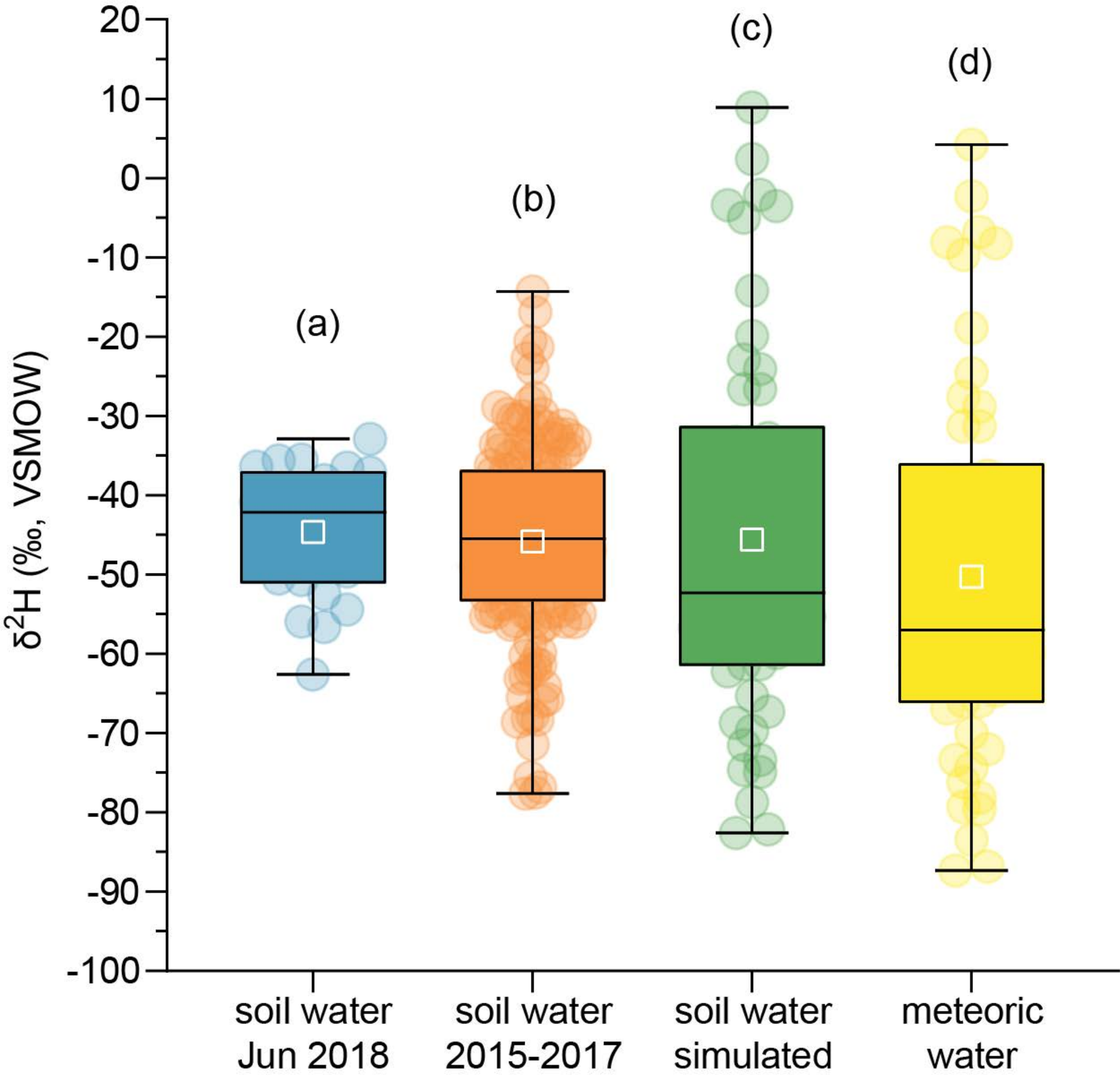
20
10
0
-10
-20
-30
-40
-50
-60
-70
-80
-90
-100
δ2H (‰, VSMOW)
(a)
(b)
(c)
(d)
soil water Jun 2018
soil water 2015-2017
soil water simulated
meteoric water